PHOTO-INDUCED REACTIONS OF A PHOTOCHROMIC FULGIDE IN POLYMER MATRICES AND IN SOLVENTS

BY

KALSOM MOHD GHAZALLI ©

A THESIS SUBMITTED TO THE DEPARTMENT OF CHEMISTRY, LAKEHEAD UNIVERSITY IN PARTIAL FULFILLMENT OF THE REQUIREMENTS FOR THE DEGREE OF MASTER OF SCIENCES

OCTOBER, 1995

THESIS SUPERVISOR: DR. M. RAPPON

DEPARTMENT OF CHEMISTRY,

LAKEHEAD UNIVERSITY,

THUNDER BAY, ONTARIO,

CANADA P7B 5E1.

ISBN 0-612-09227-5

Canada

DEDICATED TO MY PROFESSORS...

"THE RELATION BETWEEN SUPERIORS AND INFERIORS IS LIKE THAT BETWEEN WIND AND GRASS. THE GRASS MUST BEND WHEN THE WIND BLOWS OVER IT."

~CONFUCIUS~

ACKNOWLEDGEMENTS

I would like to express my deepest appreciation and thanks to all my professors at Lakehead University for their unforgettable and invaluable assistance, and their kindness shown throughout my association with them. Certainly, the learning process has always been and will remain a very meaningful experience throughout the years. Very special thanks are due to my thesis supervisor, Dr. M. Rappon, for his guidance and encouragement. He has helped me to appreciate the beauty of chemistry and provided stimulating and illuminating discussions related to the research work. His creativity and motivation have been a great encouragement and definite help on this work. I also wish to thank Mrs. Somjitt Rujimethabhas for her considerable help with the C-programming.

I am grateful to Mr. B. K. Morgan, Mr. D. Corbett, Mr. A. Bharath, Mr. A. J. Harding, and Mrs. E. Jensen for their technical assistance, to Mr. E. Drotar and Mr. R. Mazzaferro of the science workshop, and to members of staff of the science instrumentation laboratory.

The help and support of my ESL professor, Mr. David Nancekivell, and other friends during the course of this thesis preparation is greatly appreciated.

Finally, I would like to extend my deepest gratitude to the Government of Malaysia for the financial support in the form of a scholarship. I am also grateful for financial assistance from Graduate Studies and the Department of Chemistry, Lakehead University. The award of the David Jones

Silver Jubilee Scholarship is gratefully acknowledged.

TABLE OF CONTENTS

TABLE OF CONTENTS continued

TABLE OF CONTENTS continued

LIST OF TABLES

PAGE NUMBER

LIST OF FIGURES

PAGE NUMBER

LIST OF FIGURES continued

LIST OF SCHEMES

PAGE NUMBER

ABSTRACT

A photochromic fulgide, commonly known as Aberchrome 540, is amber in its ring-opened **E** [(E)-α-(2,5-dimethyl-3-furylethylidene)(isopropylidene)succinic anhydride] and **Z** [(Z)-α-(2,5-dimethyl-3-furylethylidene)(isopropylidene)succinic anhydride]. The **E** form is dispersed in various polymer matrices to form thin solid films on quartz plates by a solution-cast technique. The **E** form is photoisomerized with a u.v. light at $\lambda > 300$ nm to undergo a conrotatory ring-closure, **C** form[7,7a-dihydro-2,4,7,7,7a-pentamethylbenzo[b]furan-5,6-dicarboxylic anhydride]. The kinetics of **E** → **C** reaction are followed spectrophotometrically using λ_{max} of the **C** form at 493 nm. The reaction is studied at 303-338 K. The reaction showed two first-order processes one after another, suggesting the possible existence of two major conformers of **E** form. By the same method, the **Z** form is photoisomerized to the **C** form via the **E** form: $\mathbf{Z} \overset{k_{1B}}{\rightarrow} \mathbf{E} \overset{k_{2B}}{\rightarrow} \mathbf{C}$. The rate constant k_{1B} is obtained by fitting the experimental data with a consecutive kinetic model using previously obtained k_{2B}. The calculated k_{1B}'s and the apparent(thermal) activation energies are affected by the available free volume at the dye sites, molecular motions of the media and dipolar interactions. The polymers used are poly(styrene), poly(p-t-butyl styrene), poly(vinyl acetate), and poly(n-butyl methacrylate).

The kinetics of the **E** → **C** reaction are also

investigated in various solvents at 298-338 K. The reaction follows simple first-order kinetics with a single rate constant.

The **C** form, in poly(styrene) and poly(carbonate) films, is photobleached with a visible light source to **E** form, using a similar technique to the above, except that a cryogenic system is used to facilitate the studies at the temperature range of 83-303 K. The results show that various modes of molecular motions of the media can influence the reaction.

1 INTRODUCTION

1.1 General

There is a wide variety of organic and inorganic compounds that exhibit photochromism. The groups of organic photochromic compounds are the anils(Schiff's base), disulfoxides, hydrazones, osazones, semicarbazones, stilbene derivatives, succinic anhydrides, camphor derivatives, o-nitrobenzyl derivatives, spiropyran compounds, spiro-oxazines, and others. The inorganic photochromic compounds include metal oxides, mercury compounds, copper compounds, alkaline earth metal sulfides, transition metal compounds such as the carbonyls, and so on[1].

The photochromic processes play important roles in nature and also have potential use in several commercial applications. In nature, for example, the photoinduced isomerization of urocanic acid dissipates u.v. radiation from the sun, thus reducing its harmful effect on the skin[2]. Furthermore, sterols are isomerized to vitamin D[3], and rhodopsin in the retinal rods of the eye resolves both the colour and the intensity of the radiation[4].

The potential applications of the photochromic processes in several commercial areas will be discussed later.

1.2 Historical Background

The discovery of the photochromic materials can be traced back as far as 1876[5]. Later, over the period 1893-1911, through a series of experiment performed by Stobbe and

co-workers, a class of photochromic compounds, fulgides(derivatives of dimethylene succinic anhydride as shown in Figure 1.1[4]) were synthesized and developed. The subject was then extensively studied and reviewed by Johnson and his co-workers in 1951[6]. The word 'fulgides', originating from the Latin('fulgere'), means to glisten and shine, as these compounds often formed bright, shiny crystals[7].

Figure 1.1 Derivatives of dimethylene succinic anhydride

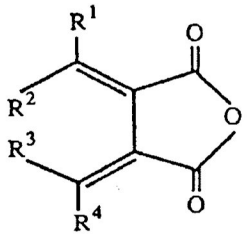

The present fulgides, which are apparently one of the oldest groups of photochromic compounds[8], continue to attract considerable attention from various groups of academic and commercial researchers. A major breakthrough in the development of fulgides was made by Heller and co-workers[9], one of the leading research groups in the field. They succeeded in synthesizing the 3-furyl fulgide compounds of

(E)-α-2,5-dimethyl-3-furylethylidene(isopropylidene)succinic anhydride, which have good photochromic properties and have a low fatigue factor.

Recently, the kinetics of photobleaching of **C** form of Aberchrome 540 in **C** → **E** reaction in annealed[10] and unannealed[11] polymer matrices have been reported from this laboratory. As part of an extension of this work, some aspects of the photochemical kinetics of some of these fulgides in solid polymer media and in solvents are reported in the present thesis.

1.3 Overview of the Commercial Importance of Organic Photochromic Compounds

Due to the advent of the new technologies, many new and exciting developments have emerged and taken place in the potential applications for photochromic materials. These materials have been extensively exploited in various photoactive devices such as erasable optical memory and imaging[12-14], electro-optic devices[15], chemical-gated molecular device[16-17](involving photoinduced change only when, for instance, its hydrogen bonds are chemically perturbed[18]), security and printing applications[19], and eyewear products[20]. Those photochromic compounds applied to such purposes, however, are limited to several molecular structures[21], such as spiropyrans[22], azo-dyes[4], fulgides[23], bisanthracenes[24], and diarylethenes[25].

On the basis of theoretical reasoning, Hirshberg[26], at the Weizmann Institute, Israel(in the mid-1950s), revealed the potential ability of photochromic compounds in an optical memory device. The information could be stored at the molecular level because individual molecules could be switched reversibly between near-colourless and highly coloured forms. The suggestion has led to more vigorous research on the subject[27]. Since 1980, the number of patents per annum for photochromic materials used as an erasable optical memory has increased by a factor of three compared with a decade ago[28]. Its density is being limited by wavelength to *ca.* 10^8 bit cm^{-2}(the theoretical storage density is proportional to $1/\lambda^2$) for a simple two-dimensional medium, or up to 10^{12} bit cm^{-3} for a three-dimensional amplitude-recording medium using two photon writing/reading[29].

There has been an increasing demand for photochromic compounds dispersed in plastic lenses. In the United States, for example, 75% of prescription lenses are now made of plastics[20]. Photochromic plastic lenses are lighter than "photogrey" glass lenses and are suitable for some prescription lenses.

The commercial significance of photochromic fulgide compounds is reflected in the number of patents filed by various countries: Great Britain, France, Germany, Holland, Hong Kong, Italy, Japan, and U.S.A[4].

1.4 Basic Principles of Photochromism

Photochromism is defined as the phenomenon whereby a single species(A) undergoes reversibly a major change in its absorption spectrum on irradiation at a wavelength(λ_1) to form a more highly coloured species(B). The species(B) reverts to a colourless state of species(A)(is called a photobleaching process) either thermally(occurring directly from the electronic ground state) or photochemically(occurring through an electronically excited state) with irradiation at a different wavelength(λ_2) as seen in Figure 1.2[30-32].

Figure 1.2 Schematic of photochromic transitions

$$\text{A(colourless)} \underset{\lambda_2 \text{ or thermally}}{\overset{\lambda_1}{\rightleftharpoons}} \text{B(coloured)}$$

Apparently, this reversible process is due to the ability of the photochromic molecules to exist in two different states whose relative concentration depends on the wavelength of the incident light[4].

Many applications of photochromic dyes are employed in solid media. Thus several investigations, related to the structural, mechanistic and kinetic aspects, are made with the photochromic dye moieties dispersed in or bound to the main-chain of solid polymer matrices[11,33]. The most important

and comprehensively studied class of photochromic dyes are the spiropyran family and its derivatives[34-43] as seen in Figure 1.3[33]. When the colourless form of a spiropyran(SP), dispersed in a polymer matrix, is irradiated with a u.v. light, it is converted to the ring-opened coloured form known as merocyanine(MC). The latter may be reverted to SP either by white light or heat and is known as a photobleaching process. Other dyes studied on the basis of such systems include azobenzene[39], 2,2' azonaphthalene[44], spiroindolinonaphthoxazine[45], etc.

Figure 1.3 Examples of photochromic spiropyran and its derivatives

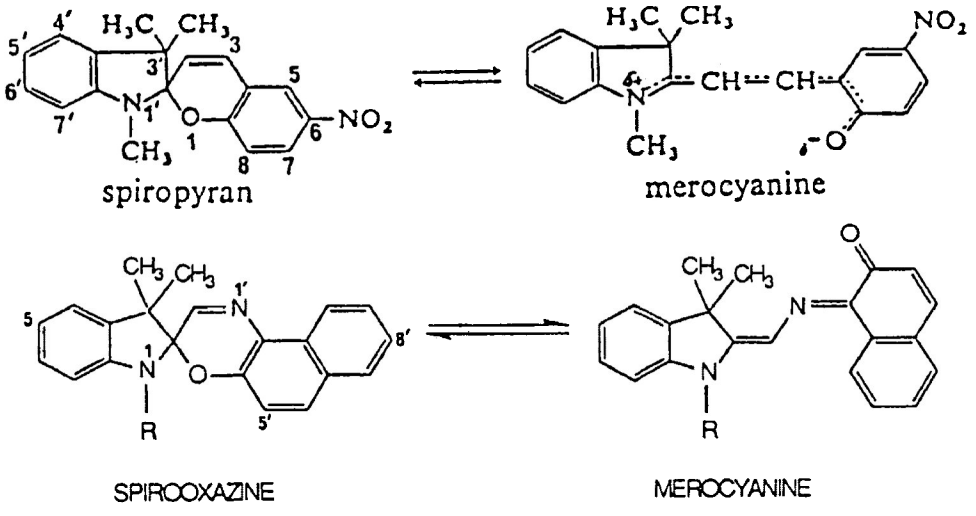

1.4.1 Free Volume Hypothesis

In order for a photochemical reaction to take place, the photochromic dye must be photo-induced or thermally induced as illustrated earlier in Figure 1.2, thus amplifying the effect of a critical free volume at the dye site to allow for the dye molecule to initiate certain modes of motions(e.g. rotation)[46]. Insufficiency of polymer free volume requires the creation of polymer molecular motions and/or the cooperative motions of the dye and the polymer to facilitate the reaction[46]. The results of the polymer free volume studies should provide information on the photo-induced reaction of the dye, e.g. the local micro-environments at the dye sites and the molecular motions of the polymer medium, as well as its impacts on the course of the dye reaction. Essentially, the local micro-environment studies are very important in that they control many physical properties of the polymers and will thereby enhance our understanding of the guest(dye)-host(polymer matrix) relationship.

There are a number of techniques used to investigate polymer free volume. One method involves the photochemical and thermal reaction of dyes dispersed in or covalently bonded to the main-chains of polymer matrices[37,40-43,47-53]. Another method consists of using various spectroscopic techniques such as positron annihilation spectroscopy[54], small-angle X-ray and neutron diffractions[55-56], ESR[57], NMR[58], fluorescent probe[59], and dielectric relaxation[60].

In addition, theoretical studies[61-65] and atomistic modeling of polymer free volume have also been carried out[66]. Despite these efforts, our knowledge of polymer free volume is still limited. This is due to the fact that polymer free volume is dependent on the thermal and mechanical history of a sample[46].

1.4.2 Fundamental Kinetics

While the kinetic studies of the photo-induced reactions of some dyes in solutions are better known[67-69], the corresponding kinetics in solid polymer matrices are not well understood[11] such as in the case of spiropyran dyes[70]. This is because the kinetics of the photo-induced or thermal isomerization of a dye in a solution often obey a simple first-order reaction, thus enabling the extraction of the kinetic parameters; however, the very same reaction of the dye, in solid polymer matrices, often deviates from a simple first-order kinetic[11]. This is ascribed to the distinctive features of solid polymer media, the existence of the so-called kinetically inequivalent sites in the polymer[71], and/or the plausible presence of more than one conformer of the reactant, causing complications in the kinetic analyses[11,70]. Analyses of such kinetic results, however, can be made by fitting some of the experimental data on the chemical reactions in restricted media using various kinetic schemes given as follow: composite exponential

decay[40], dispersive processes[45,72-73], and kinetic matrix effect[36]. Some of these points are further discussed herein.

There are several possible causes for the deviation from the linearity of the first-order plots. The first factor is the existence of polymer free volume at the dye sites. If, for example, the free volume at the dye site is less than the critical free volume required for the dye molecules to undergo the photo- or thermal isomerization, then the molecular motion of the polymer is required in order to create a sufficient free volume for the reaction to occur. Isomerization can also take place with the cooperative motion between the dye and the polymer molecules. In this way, the reaction kinetic is greatly affected by the molecular motions of the polymer. The kinetic matrix effect has been used to deal with this situation[36]. Thermal cis-trans isomerization of azobenzene in polymer matrices[36,74] and azobenzene derivatives in poly(styrene)[75] are influenced by the free volume effect.

The second factor is the presence of more than one conformer of the reactant trapped in a solid polymer matrix. Each conformer reacts at its own rate. Thus, the composite exponential decay model[40] is better suited for this type of reaction. It is thought that the thermal bleaching of the coloured merocyanine form of the spiropyran dispersed in[34] or bonded to a main-chain polymer matrix[47,76] is likely to be influenced by this factor.

The third factor, interestingly enough, consists of the existence of strained or hindered reactant in a solid polymer matrix. Such a proposal reinforces the validity of the deviation from the first-order plot that occurred in the thermal cis-trans isomerization of azobenzene in which the cis-form was prepared under a u.v. light[74,77].

1.4.3 Structural and Mechanistic Aspects of A Photochromic Fulgide

Photochromism has been observed in crystals, solutions, polymers and glasses over a wide range of temperatures and conditions. Such a phenomenon is subjected to a range of steric and electronic effects, which allow the photochromic properties to be modified by molecular design and tailoring[4]. The present work deals with the photochromic phenomena in selected sets of polymers and in various solvents.

One fulgide used is Aberchrome 540 - typically a yellow or amber crystal of the ring-opened forms(**Z** and **E** forms) which changes to the red ring-closure form(**C** form) upon irradiation with a u.v. light. The intense red reflects the high quantum yield value(Φ = 0.23) in the photocolouration of the **E** form into the **C** form of the dye in ethanol[78]. Thus, the characteristics of high quantum yield possessed by Aberchrome 540 make photochromic fulgide one of the most efficient and promising[79] compounds applicable to

information data storage, as discussed earlier.

Yoshioka and co-workers[80] report that the ring-opened **C** form of the dye is non-planar, with the torsional angle of -39.6°C between the α-C(of the ethylidene)-C(of succinic anhydride) and the α'-C(isopropylidene)-C(of succinic anhydride). Apparently, there is too much steric-crowding between the succinic anhydride and the furan ring(planar structure is retained) causing the large deviation from planarity for the succinic anhydride moiety. Note that in Scheme 1, the bond distance between the C-2 of the furan ring and the α'-C of the isopropylidene(which are the two carbons that join to form the six-membered ring during photocyclization) is 3.44 Å. They also report that the molecular structure reveals that the π-conjugation does not exist between the anhydride and the furan ring.

Scheme 1 Aberchrome 540

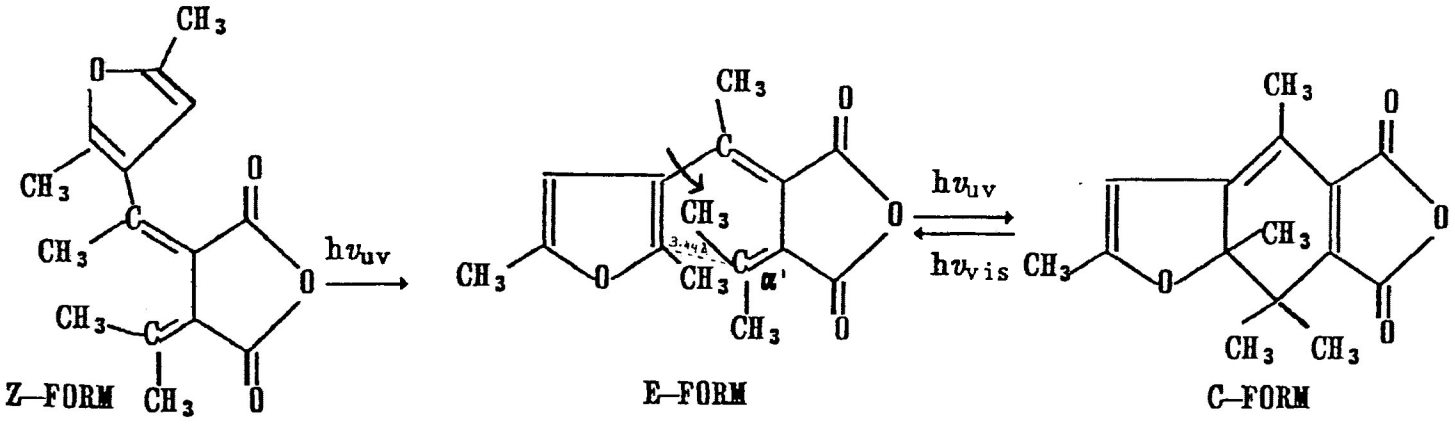

Heller et al.[81] hypothesizes that the photocyclization reaction of **E** → **C** occurs by n-π^* excitation of one of the carbonyl chromophores in the molecule. The mechanism indicates that the photochromic process is an electrocyclic reaction in accordance with the Woodward-Hoffman selection rules. However, Lenoble and Becker[82] suggest that the excitation of π-π^* singlet excited states is responsible for the photochromic reaction, i.e.[83] a $\pi \rightarrow \pi^*$ singlet excitation is the decisive state for the photochromic ring-closure reaction. In another study[84], Yoshioka and Irie found that the ring-closure red form(**C** form) dye is of lower energy than the ring-opened amber form(**E** form). This suggests that the final form during photoisomerization or photocolouration of Aberchrome 540 is the **C** form, the most stable and favored form to exist which is observed in the present work.

1.5 Purposes of the Present Study

There are some unresolved problems of previous photochromic reactions in solid polymer media, e.g. the causes of deviation from linearity of the first-order plots. It is not clear whether such deviation is brought about by the rigidity of the polymer media or by the presence of more than one conformer of the reactant, as mentioned earlier. Unfortunately, some of the dyes used in the previous work, especially merocyanine(MC), the coloured form of

spiropyran(SP), may exist in several conformers[34] and their size is large enough to be affected by the rigidity of the media. Thus, such dyes are not a suitable choice for resolving the above problems.

It has been found, from this laboratory, that the ring-closure **C** form of Aberchrome 540(in which only one conformer exists), when reacted in annealed[10] and unannealed[11] polymer matrices, yields simple first-order plots. It appears that the molecular size of the dye is small enough not to be influenced by the rigidity of the media. Therefore, various forms of Aberchrome 540 are suitable candidates to investigate the corresponding kinetics in selected media so that some of the problems mentioned earlier can be resolved.

The purposes of this experiment are outlined herein.

A)The kinetics of photocolouration of the **E** form(**E** → **C**) in selected solvents. A recent report[46] on the **E** → **C** reaction in solid polymer matrices indicated that two major conformers of the **E** forms could be trapped in a solid polymer matrix and that one conformer reacts first, followed by the second one. Thus, the first-order plot shows two distinct slopes, one after another[46]. The purposes of reacting the **E** form in solvents are twofold: first, to compare the reaction with that in rigid polymer media, and second, to determine whether the specific solvent effects, such as polarity, viscosity or hydrogen bonds, have any impact on the reaction

kinetics.

B)The photoisomerization of **Z** → **E** of the **Z** form in selected polymer matrices. One of the goals of this experiment is to extract the rate constants and the apparent(thermal) activation energies(E_a) of the reaction. Another purpose is to examine whether the sweeping motion of the furan moiety(which is required in the course of the reaction **Z** → **E**) can be influenced by the rigidity of the polymer matrix.

C)The photobleaching or photodecolouration of the same dye in the reaction **C** → **E** in polymer matrices and the photodecolouration is conducted under cryogenic conditions. The purpose of this experiment is to study whether some of the molecular motions of the polymer media, such as the **β** or the **γ** relaxations, could affect the kinetics of the photoisomerization. Poly(carbonate) and poly(styrene) matrices are chosen because their physical properties, such as molecular motions, are reported in the literature[75,85].

2 EXPERIMENTAL PROCEDURES

2.1 Photo-Induced Reactions of A Dye in Polymer Matrices and in Solvents

2.1.1 Materials and Sample Preparation

A Photocolouration of E → C of Aberchrome 540 in Solvents

In this experiment, reaction mixture consisting of **E** form dye and selected solvent were prepared. A number of solvents with different $E_T(30)$ values, which are the empirical parameters of solvent polarities were reported in Table 2.1. For comparison, some other physical properties of the solvents, such as relative permittivity(ϵ_r), dipole moment(μ), and viscosity(η) were also collected in Table 2.1[86]. The mixture was placed in a quartz cell(thickness ~1 cm) containing a small magnetic stirrer, which helped to get a well-mixed solution. The cell was then placed in a heating block whose temperature was regulated and controlled to ±0.3 K. It was then irradiated at various irradiation times with a u.v. lamp(Black Rays), transmitting only $\lambda > 300$ nm. The extent to which the red dye was formed at each irradiation time was monitored at λ_{max}=493 nm with a spectrophotometer(Perkin Elmer λ 11). It is important to mention that the distance between the lamp and the reactor was fixed to ensure the uniform performance resulting in the constant output(the fixed distance between the lamp and the reactor was also done in experimental sections B and C). During the autozero(background) correction of the

spectrophotometer, the measurement of the absorption is due to the reference(in this case the cuvette and the appropriate solvent). This absorption is substracted automatically during sample(dye and solvent) measurement to present the absorption of the dye alone. The experiment was performed at 298-338 K.

Table 2.1 **E** form dye in selected solvents[a] with various polarity

Solvent	Relative permitti-vity, ϵ_r[b]	Dipole moment, μ[c] (10^{-30}Cm)	Solvent polarity parameter, $E_T(30)$[d] (kJ mol^{-1})	Viscosity, η[e](mPas)	Concentr-ation of dye (M)
Cyclo-hexane	2.02	0.0	129.3	0.894[f]	7.69 x 10^{-5} M
n-Heptane	1.92 (293 K)	0.0	130.1	0.386	9.23 x 10^{-5} M
Toluene	2.38	1.0	141.8	0.568[g]	2.28 x 10^{-5} M
Ethyl acetate	6.02	6.1	159.4	0.423[h]	7.69 x 10^{-5} M
Chloro-form	4.81 (293 K)	3.8	163.6	0.542	-Same as above-
t-Pentanol	5.78	5.7	172.0	3.706[h]	-Same as above-

Table 2.1 continued

Solvent	Relative permittivity, ϵ_r[b]	Dipole moment, μ[c] (10^{-30}Cm)	Solvent polarity parameter, $E_T(30)$[d] (kJ mol^{-1})	Viscosity, η[e] (mPas)	Concentration of dye (M)
Acetonitrile	35.94	11.8	190.8	0.345	-Same as above-
Ethanol	24.55	5.8	217.1	1.074[f]	-Same as above-

[a]All values are at 298 K, unless stated otherwise.

[b]Relative permittivities taken from A. A. Maryott and E. R. Smith: Table of Dielectric Constants of Pure Liquids, NBS Cicular 514, Washington(1951).

[c]From A. L. McClellan: Tables of Experimental Dipole Moments, Freeman, San Francisco(1963).

[d]Converted from $E_T(30)$ in kcal mol^{-1} of C. Reichardt: Solvents and Solvent Effects in Organic Chemistry, 2nd ed., VCH, Weinheim(1988). Conversion factor:1 kcal mol^{-1} =4.184 kJ mol^{-1}.

[e]Unless specified otherwise, values are taken from R. C. Weast(ed): Handbook of Chemistry and Physics, 66th ed., CRC Press, Boca Raton, Florida(1985/86).

[f]D. R. Lide and H. P. R. Frederikse(eds): Handbook of Chemistry and Physics, 76th ed., CRC Press, Boca Raton, Florida(1995/96).

[g]Interpolated from data given in note [e](above).

[h]Interpolated from E. W. Washburns(ed): International Critical Tables, Vol VII, Mc Graw Hill, New York(1930).

B Photoisomerization of **Z** → **E** of Aberchrome 540 in Solid Polymer Matrices

These experiments deal with the photoisomerization reaction in solid polymer matrices. Poly(styrene)(PS), poly(p-t-butyl styrene)(PTBS), poly(n-butyl methacrylate)(PNBMA), and poly(vinyl acetate)(PVAC) were purchased from Polysciences Inc. Each polymer was further purified by the precipitation method[87]. During the initial stage of the purification method, the polymers were dissolved in good solvents(e.g. methylene chloride) and then the polymers were precipitated with the poor solvents. Information regarding the molecular weights, glass-transition temperatures, T_g's[11] and appropriate solvents[88] for purifying purposes for all the polymers are listed in Table 2.2. The molecular weights of PS and PVAC were reported by Polysciences Inc. and those of PTBS, PNBMA and PC were determined by viscometry. The T_g's of the various polymers were determined by the Differential Scanning Calorimetry(DSC). Prior to use, all the solvents were dried in molecular sieves and distilled, collecting only the middle fractions.

Table 2.2 Average molecular weight of polymers

Polymer	Molecular weight,M	T_g (K)	T_g (°C)	Good solvent	Non-solvent
PS	275,000	373	100	methylene chloride/ toluene	cyclo-hexanol
PTBS	20,000	403	130	methylene chloride/ toluene	methanol
PNBMA	73,000	307	34	methylene chloride/ toluene	methanol
PVAC	90,000	302	29	methylene chloride/ toluene	cyclo-hexanol
PC	34,000	418	145	methylene chloride	heptane

Solid film samples (thickness ~ 20μm) were prepared by solution-casting on quartz plates. Each mixture was made up of 7% polymer dissolved in methylene chloride and 1% of dye(**Z** form) relative to polymer. This step was done carefully to ensure the homogeneity of the dispersed dye in polymer solution on the plate. The films were dried under vacuum to remove traces of solvent.

Each thoroughly dried sample film was placed in a heating block whose temperature was regulated and controlled to ± 0.3 K. It was then irradiated at various times with a u.v. lamp(Black Rays) equipped with a glass filter, transmitting only $\lambda > 300$ nm. The extent to which the red dye

was formed at each irradiation time was monitored at λ_{max} = 493 nm with a spectrophotometer(Spectronics 2000, Bausch & Lomb). Prior to use, the u.v. spectrophotometer was warmed for at least two hours to get an optimum performance. The experiments were carried out at the temperature range of 303 to 338 K. The incident intensity of the u.v. lamp as measured with a chemical actinometer(by using Aberchrome 540[89])was determined to be 1.1×10^{-8} einstein/cm^{2}sec at the power output of 100 W. Previous applications of this chemical actinometer were found to be satisfactory[90-92].

C Photobleaching of **C** → **E** of Aberchrome 540 in Solid Polymer Matrices at Low Temperatures

In this experiment, the solid polymer matrices were prepared in the same way as described in section B. Having accomplished this step, then the sample was loaded in a cryogenic dewar. This time, the polymers employed were poly(styrene) and poly(carbonate) of bisphenol A. The reaction was studied by monitoring the absorbance of the **C** form at λ_{max} = 493 nm over the temperature range of 83-303 K.

To facilitate the investigation at low temperatures, a cryogenic system described in Figure 2.1 is required. It was constructed from a dewar(JANIS VPF - 100 Dewar) equipped with four quartz windows. The common end of a bifurcated quartz fibre optic bundle(Oriel) was positioned at one window. On one of the separated ends, visible light(from a General

Electric tungsten lamp, 75 W) was piped in as an irradiation light source. Another separated end was used to pipe in the analytical light at λ = 493 nm from a monochromator(UNICAM). The light passed through the sample, held in a sample holder whose temperature was regulated and controlled to ±0.3 K. The analytical light leaving the sample went to the opposing window and was measured with a photodiode detector, whose output was preamplified. Then the amplified signal was fed into a lock-in amplifier(Stanford Research SR510).

With the analytical light source blocked off(with a shutter), the sample was irradiated with the visible light at various times. Following each irradiation time, the visible light was blocked off, the analytical light was allowed to pass through the sample and the transmitted light was detected by the photodiode. The power output of the light source intensity was determined by using a power-meter (model 1825-C, Newport) and was found to be 10.1 nW.

Figure 2.1 Schematic diagram of cryogenic system

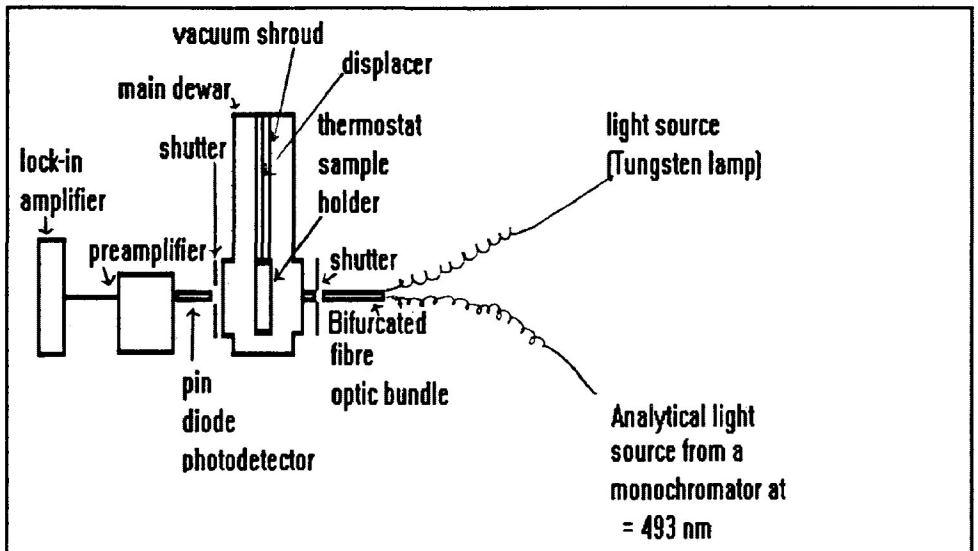

Experimental Set-up:

The light signals were recorded by lock-in-amplifier. The temperature of the system was regulated and controlled by liquid nitrogen in the main dewar of the vacuum shroud and the heated resistance wire embedded in the sample holder. The displacer in the main dewar can be positioned to get sample temperature between 83-303 K for this work. Main dewar must be warmed to room temperature between -280 to 310 K by simply allowing the liquid nitrogen to boil away to avoid from contaminating the vacuum space before opening the vacuum jacket[93].

3 EXPERIMENTAL RESULTS

3.1 Photo-Induced Reactions of A Dye in Polymer Matrices and in Solvents

3.1.1 Kinetic Analysis

A Photocolouration of **E** → **C** of Aberchrome 540 in Solvents

i) Absorbance Plot

The following is the photocolouration reaction of Aberchrome 540 from ring-opened(**E** form) to ring-closure(**C** form) under the u.v. radiation:

$$\mathbf{E} \xrightarrow{h\upsilon_{uv}} \mathbf{C}$$

Initially	a_0 amount of **E** form presents	zero amount of **C** form
At time,t	x amount of **E** form reacts	x amount of **C** form presents
At time,t	$(a_0 - x)$ amount of **E** form remains	(x) amount of **C** form presents

Note that x is a variable

Then the rate of dye(**E** form) reacts is expressed as:

$$-\frac{d[E]}{dt} = \frac{d[C]}{dt}$$

$$= k[E]$$

$$= k[a_0 - x]^p \text{---} (1).$$

If p=1, then k is known as the pseudo first-order rate constant. For convenience, the rate equation (1) can be written as

$$\frac{dx}{dt}=k(a_0-x),$$

and is integrated with respect to time,t, to get

$$\int\frac{dx}{(a_0-x)}=\int kdt---(2).$$

Since x amount of **E** form reacts to produce x equivalent amount of **C** form, then integration of equation (2) results in

$$-\int\frac{d(a_0-x)}{(a_0-x)}=\int kt$$

and becomes

$$-\ln(a_0-x)=kt+constant---(3).$$

At time,t = 0, x = 0 and equation (3) equals to

$$-\ln a_0=constant.$$

Thus

$$-\ln(a_0-x) = kt - \ln a_0 \quad ---(4)$$

is derived. Multiply both sides of equation (4) by (-) and it becomes the general form for the kinetic equation of the photocolouration of **E** → **C**:

$$\ln(a_0-x) = -kt + \ln a_0$$

equivalent to

$$\ln([A_\infty - A_0] - [A_t - A_0]) = -kt + \ln(A_\infty - A_0) \quad ---(5).$$

In a simplified form, equation (5) can be reduced to

$$\ln(A_\infty - A_t) = -kt + \ln(A_\infty - A_0) \quad ---(6).$$

In this present work, after each irradiation with a u.v. light at increasing exposure times, the change in absorbance allows for the rate constant calculations. The plots of $\ln(A_\infty - A_t)$ against time,t are linear for all the temperatures studied. Note that A_0, A_t, and A_∞ correspond to the absorbance of the red dye(**C** form) at time zero, at any time,t, and at a sufficiently long time approaching maximum conversion,

respectively. The rate constant k in equation (6) is replaced with k_{1A} in this section(A).

Table 3.1 presents a list of rate constant values(in 10^{-2} s^{-1}) for k_{1A} at 298-338 K for the dye reaction in various solvents. The correlation coefficient is better than 0.98 for the dye reaction in all solvents studied except the correlation coefficient is between 0.96-0.97 for the same reaction in chloroform.

Figures 3.1-3.16 are plots of $\ln(A_\infty - A_t)$ of Aberchrome 540 in red **C** form against time(min.) in various solvents at the specified temperatures. Figure 3.17 shows typical absorption spectra of **E** form dye in liquid chloroform, indicating the existence of the isosbestic points for the first-order transformation in organic solvents. A special feature of the dye reaction as presented in Figures 3.1-3.16 is typified by one distinct slope, which is observed in all solvents studied as compared to two distinct slopes in polymer matrices studied previously[46]. The one distinct slope allows for the extraction of the apparent first-order rate constants: k_{1A} occurs approximately 5 minutes of the total irradiation times.

Table 3.1 Tabulated data for rate constants k_{1A} in various solvents

Temperature (K)	Solvent	Rate constant, k_{1A} (10^{-2} s^{-1})
298	Cyclohexane	0.82
	n-Heptane	0.84
	Toluene	0.90
	Ethyl acetate	0.88
	Chloroform	2.21
	t-Pentanol	0.88
	Acetonitrile	0.92
	Ethanol	1.30
303	Cyclohexane	0.92
	n-Heptane	0.80
	Toluene	0.84
	Ethyl acetate	0.86
	Chloroform	1.10
	t-Pentanol	0.93
	Acetonitrile	0.82
	Ethanol	1.36

Table 3.1 continued

Temperature (K)	Solvent	Rate constant, k_{1A} (10^{-2} s^{-1})
308	Cyclohexane	0.86
	n-Heptane	0.80
	Toluene	0.90
	Ethyl acetate	0.76
	Chloroform	1.49
	t-Pentanol	0.91
	Acetonitrile	0.81
	Ethanol	1.75
313	Cyclohexane	0.84
	n-Heptane	0.76
	Toluene	0.84
	Ethyl acetate	0.79
	Chloroform	1.43
	t-Pentanol	0.89
	Acetonitrile	0.86
	Ethanol	1.11

Table 3.1 continued

Temperature (K)	Solvent	Rate constant, k_{1A} (10^{-2} s^{-1})
318	Cyclohexane	0.81
	n-Heptane	0.74
	Toluene	0.88
	Ethyl acetate	0.77
	Chloroform	1.50
	t-Pentanol	0.83
	Acetonitrile	0.88
	Ethanol	1.84
323	Cyclohexane	0.81
	n-Heptane	0.78
	Toluene	0.86
	Ethyl acetate	0.86
	Chloroform	1.53
	t-Pentanol	0.91
	Acetonitrile	0.82
	Ethanol	1.63

Table 3.1 continued

Temperature (K)	Solvent	Rate constant, k_{1A} (10^{-2} s^{-1})
328	Cyclohexane	0.93
	n-Heptane	0.79
	Toluene	0.83
	Ethyl acetate	0.81
	Chloroform	0.88
	t-Pentanol	0.85
	Acetonitrile	0.81
	Ethanol	1.68
333	Cyclohexane	0.80
	n-Heptane	0.67
	Toluene	0.92
	Ethyl acetate	0.79
	Chloroform	1.16
	t-Pentanol	0.88
	Acetonitrile	0.79
	Ethanol	0.94

Table 3.1 continued

Temperature (K)	Solvent	Rate constant, k_{1A} (10^{-2} s^{-1})
338	Cyclohexane	0.91
	n-Heptane	0.73
	Toluene	0.83
	Ethyl acetate	0.78
	Chloroform	1.04
	t-Pentanol	0.88
	Acetonitrile	0.88
	Ethanol	0.96

Figure 3.1 Plot of $\ln(A_\infty - A_t)$ of red Aberchrome 540(**C** form) against time(min) at 298 K in cyclohexane

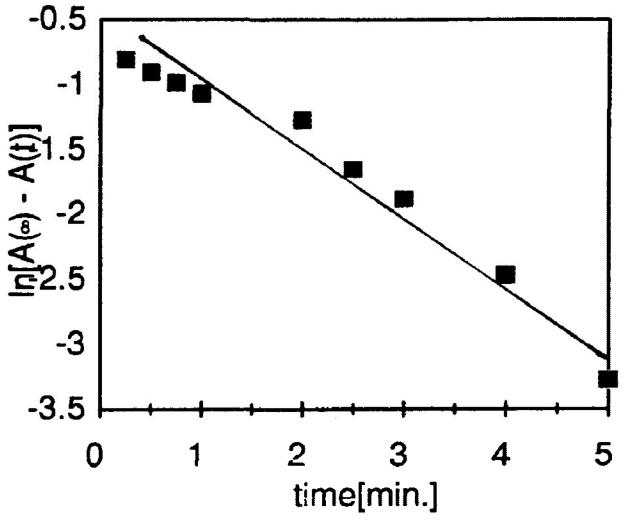

Figure 3.2 Plot of $\ln(A_\infty - A_t)$ of red Aberchrome 540(**C** form) against time(min) at 303 K in cyclohexane

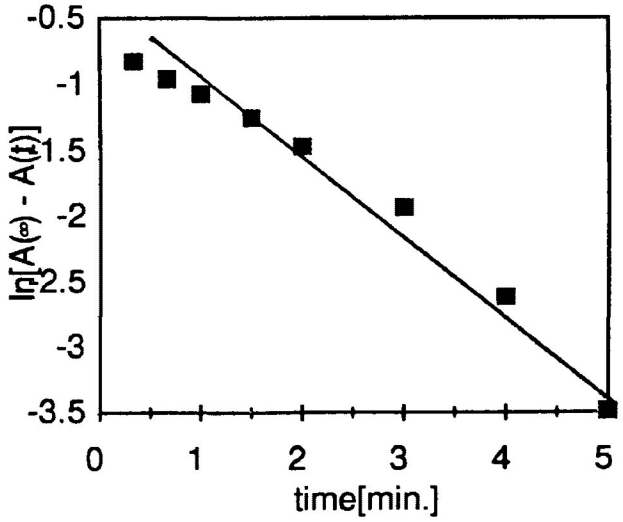

Figure 3.3 Plot of $\ln(A_\infty - A_t)$ of red Aberchrome 540(C form) against time(min) at 298 K in n-heptane

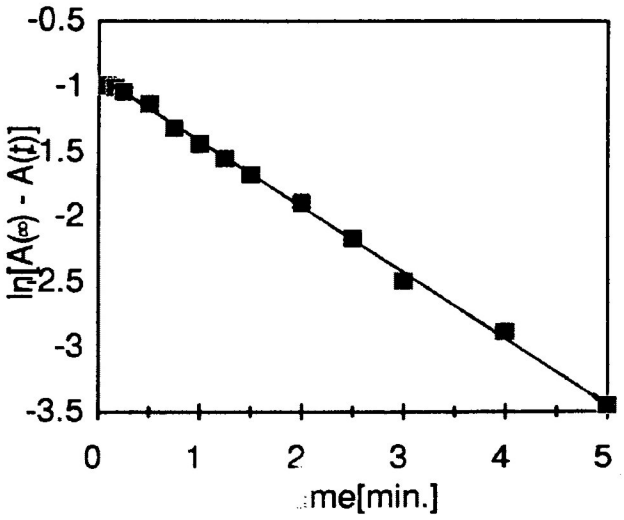

Figure 3.4 Plot of $\ln(A_\infty - A_t)$ of red Aberchrome 540(C form) against time(min) at 303 K in n-heptane

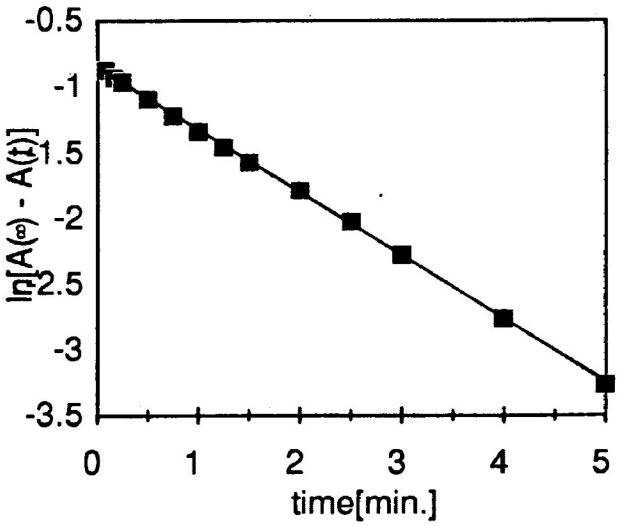

Figure 3.5 Plot of $\ln(A_\infty - A_t)$ of red Aberchrome 540(C form) against time(min) at 298 K in toluene

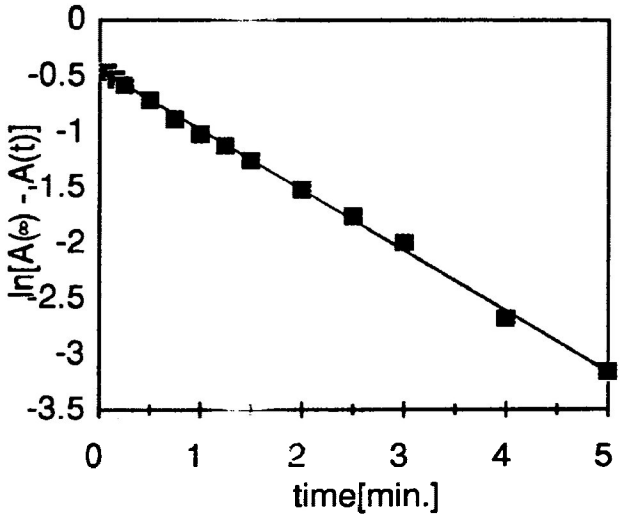

Figure 3.6 Plot of $\ln(A_\infty - A_t)$ of red Aberchrome 540(C form) against time(min) at 303 K in toluene

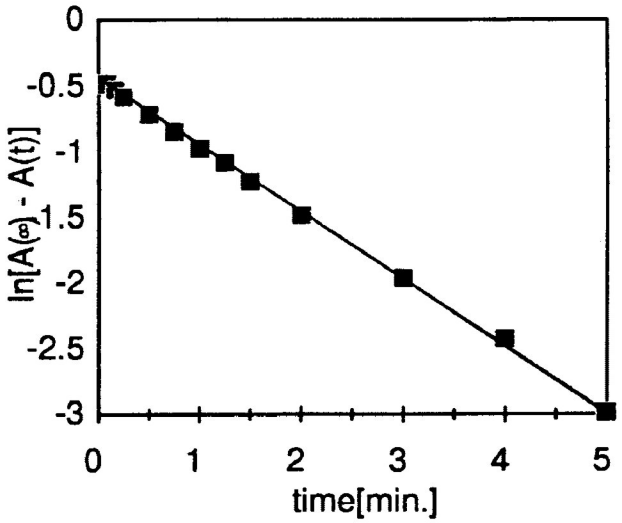

Figure 3.7 Plot of $\ln(A_\infty - A_t)$ of red Aberchrome 540(**C** form) against time(min) at 298 K in ethyl acetate

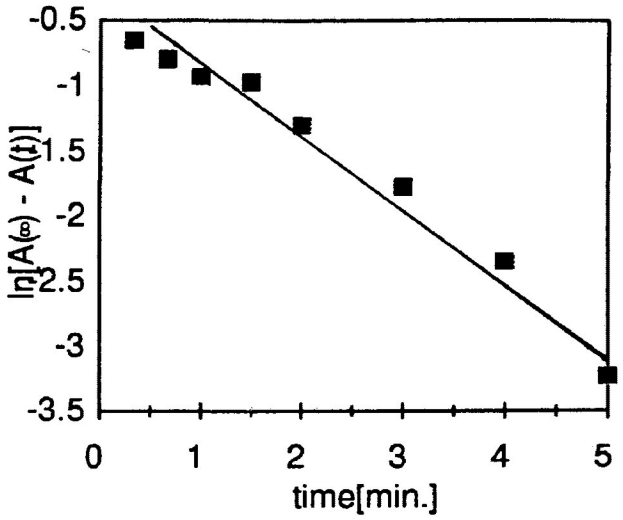

Figure 3.8 Plot of $\ln(A_\infty - A_t)$ of red Aberchrome 540(**C** form) against time(min) at 303 K in ethyl acetate

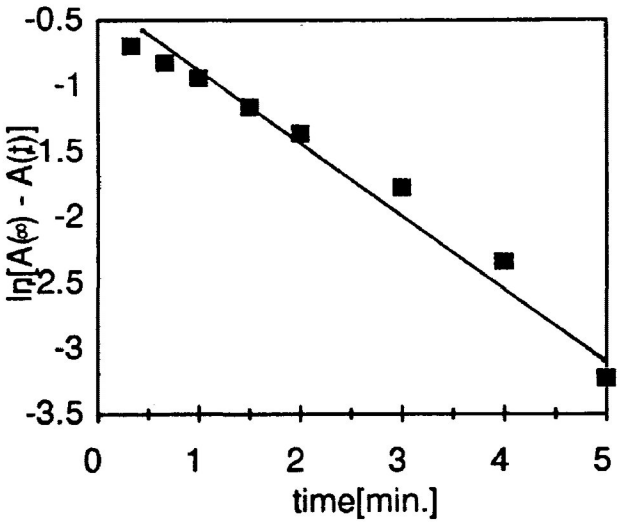

Figure 3.9 Plot of $\ln(A_\infty - A_t)$ of red Aberchrome 540(C form) against time(min) at 298 K in chloroform

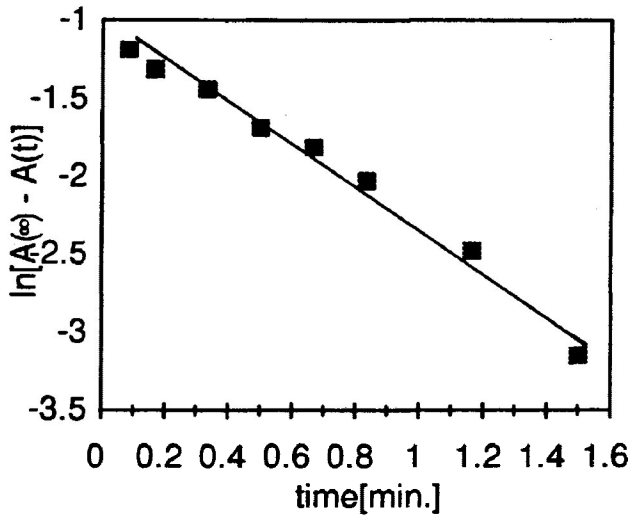

Figure 3.10 Plot of $\ln(A_\infty - A_t)$ of red Aberchrome 540(C form) against time(min) at 303 K in chloroform

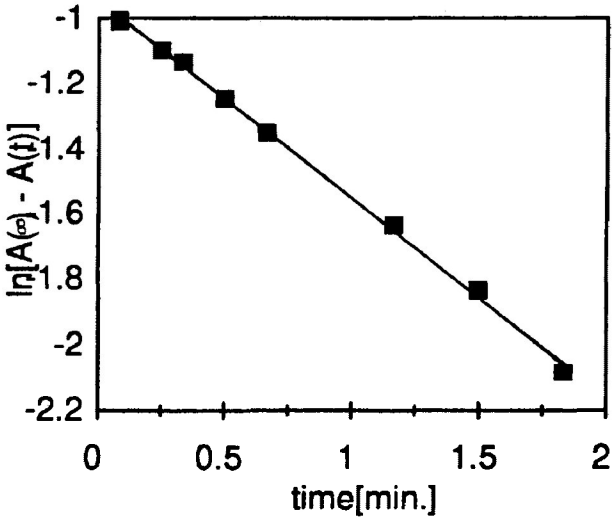

Figure 3.11 Plot of $\ln(A_\infty - A_t)$ of red Aberchrome 540(C form) against time(min) at 298 K in t-pentanol

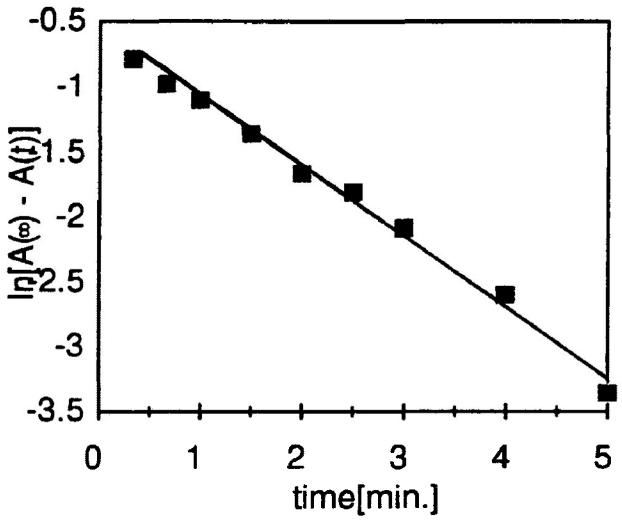

Figure 3.12 Plot of $\ln(A_\infty - A_t)$ of red Aberchrome 540(C form) against time(min) at 303 K in t-pentanol

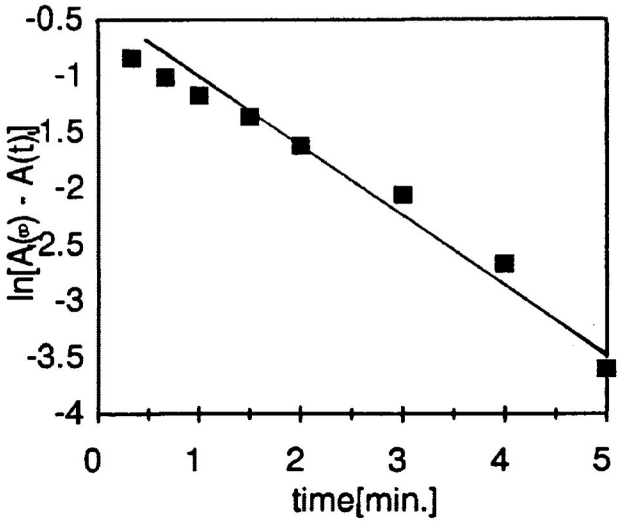

Figure 3.13 Plot of $\ln(A_\infty - A_t)$ of red Aberchrome 540(**C** form) against time(min) at 298 K in acetonitrile

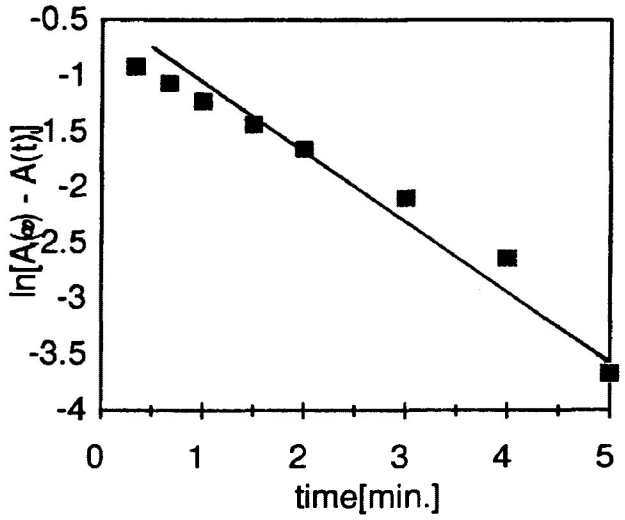

Figure 3.14 Plot of $\ln(A_\infty - A_t)$ of red Aberchrome 540(**C** form) against time(min) at 303 K in acetonitrile

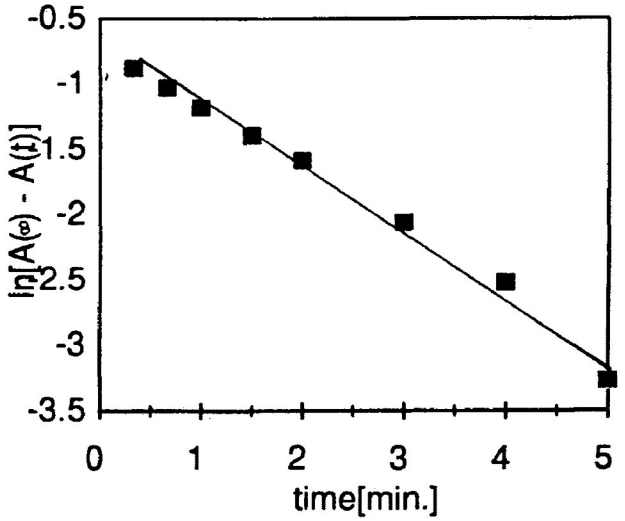

Figure 3.15 Plot of $\ln(A_\infty - A_t)$ of red Aberchrome 540(**C** form) against time(min) at 298 K in ethanol

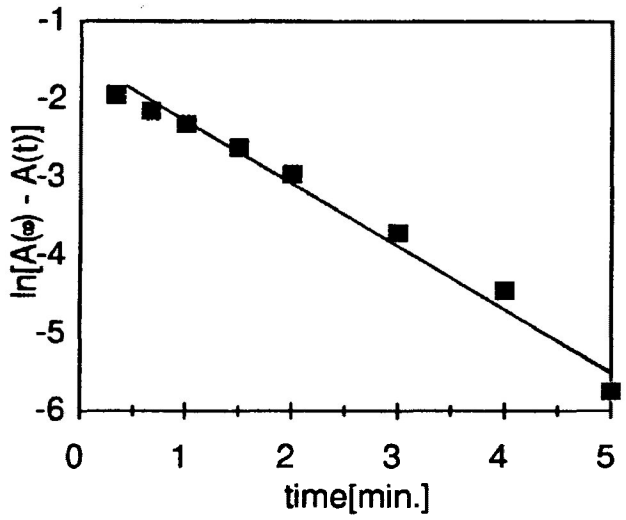

Figure 3.16 Plot of $\ln(A_\infty - A_t)$ of red Aberchrome 540(**C** form) against time(min) at 303 K in ethanol

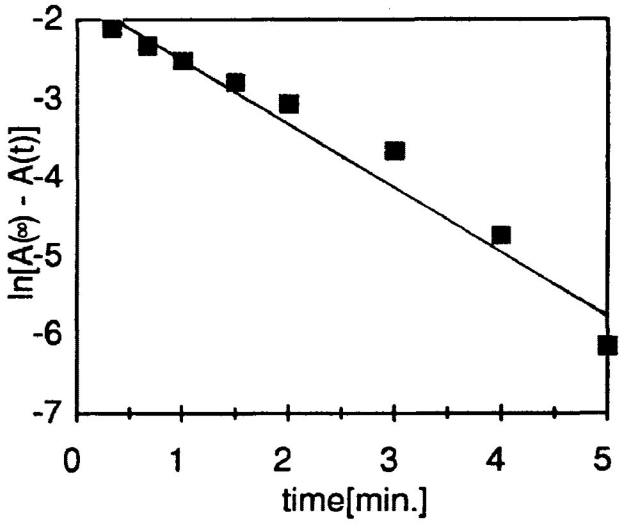

Y: echcl311; 650.0 - 350.0 nm; pts 301; int 1.00; ord 0.0100 - 0.3830 A

Inf: Figure 3.17 Absorption spectra of E form dye in chloroform

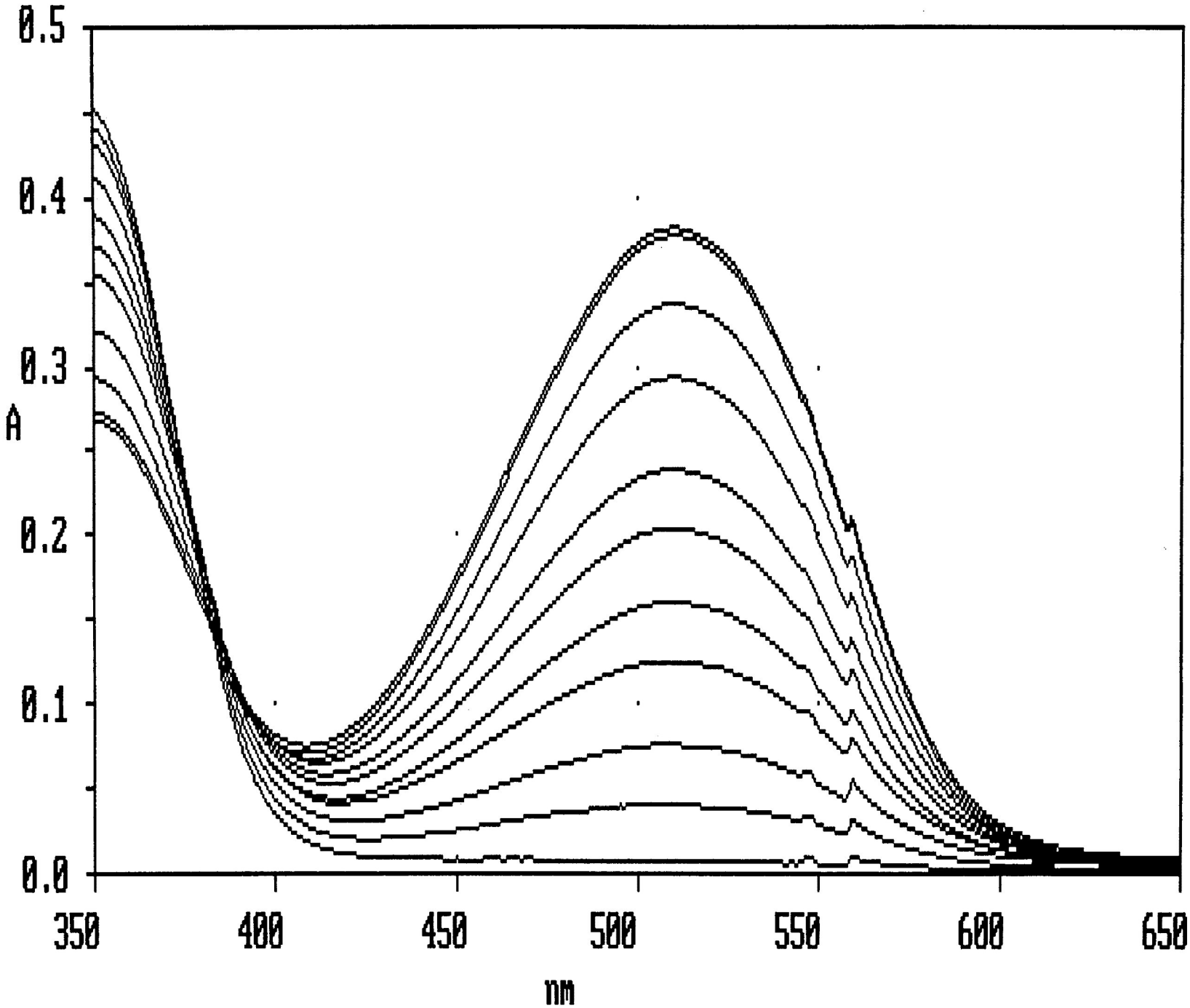

ii) Arrhenius Plot

The Arrhenius equation is given as

$$k = Ae^{-\frac{E_a}{RT}} \text{---(7)},$$

where k is the reaction rate constant, A is the Arrhenius preexponential factor, E_a defines the activation energy, R is a molar gas constant, 8.3145 $JK^{-1}mol^{-1}$ and T is the temperature in Kelvin. To obtain the Arrhenius plot, the natural logarithm on both sides of the equation (7) gives

$$\ln k = -\frac{E_a}{R} x \frac{1}{T} + \ln A \text{---(8)}.$$

The linear plot of ln k(k in s^{-1}) vs. $1/T(K^{-1})$ produces a slope of $-E_a/R$, hence the apparent overall(thermal) activation energy can be determined. In this experiment, the apparent overall(thermal) activation energies, E_a obtained from k_{1A} values as a function of temperatures in various solvents cannot be determined. This is because the differences between k_{1A} values at various known temperatures are small. Thus the calculations of each of the E_a values for various solvents would be less meaningful. Details about the differences in

k_{1A} values will be discussed later. Nevertheless, the Arrhenius equation is applicable to the experimental part of section C of this present work.

iii) Incident Intensity of U.V. Lamp with a Chemical Actinometer

The concentration of the dye(**E** form) is proportional to the absorbance(A), where A is defined as $A = \ln(I_0/I) = \epsilon c \ell$. Note that I_0 and I are the intensity of the incident light and intensity of transmitted light by the sample respectively. ϵ is the molar absorption coefficient, c is the concentration of absorbing molecules and ℓ is the pathlength of the sample(1 cm). The intensity of the incident light, I_0, also known as the radiant flux[89], can be determined from the following expression:

$$I_0 = \frac{\Delta A . V . N}{1 cm . \Phi . \epsilon . t} photon . s^{-1} \text{---(9)},$$

where N is the Avogadro's number, 6.023×10^{23} mol^{-1}, Φ is the quantum yield for photocolouration of **E** → **C**(0.20 for irradiation at 366 nm in toluene), and the definition of ϵ is retained as above(ϵ=8200 at 494 nm for toluene solutions).

In the present work, the incident intensity of the u.v. lamp measured with a chemical actinometer was found to be 1.1×10^{-8} einstein/cm^2sec, as reported earlier(section 2B).

The absorption spectra of **E** form dye in toluene using a chemical actinometer are shown in Figure 3.18. The calculation of the incident intensity of the u.v. lamp used is shown as follows:

$$I_0 = \frac{\Delta A.V.N}{1cm.\Phi.\epsilon.t}$$

$$= \frac{0.3x2.8x10^{-3}dm^3x6.023x10^{23}mol^{-1}}{0.2x1cmx8200dm^3mol^{-1}cm^{-1}x45sec}$$

$$= \frac{6.86x10^{15}photon.sec^{-1}}{N_A}$$

$$= 1.1x10^{-8}einstein/sec.$$

Since the surface area is 1 cm^2, the incident intensity of the u.v. lamp used is

$$I_0 = \frac{1.1x10^{-8}einstein/sec}{1cm^2}$$

$$= 1.1x10^{-8}einstein/cm^2sec.$$

Y: ec32; 650.0 - 350.0 nm; pts 151; int 2.00; ord 0.0311 - 0.9644 A

Inf: Figure 3.18 Absorption spectra of E form dye in toluene(actinometry)

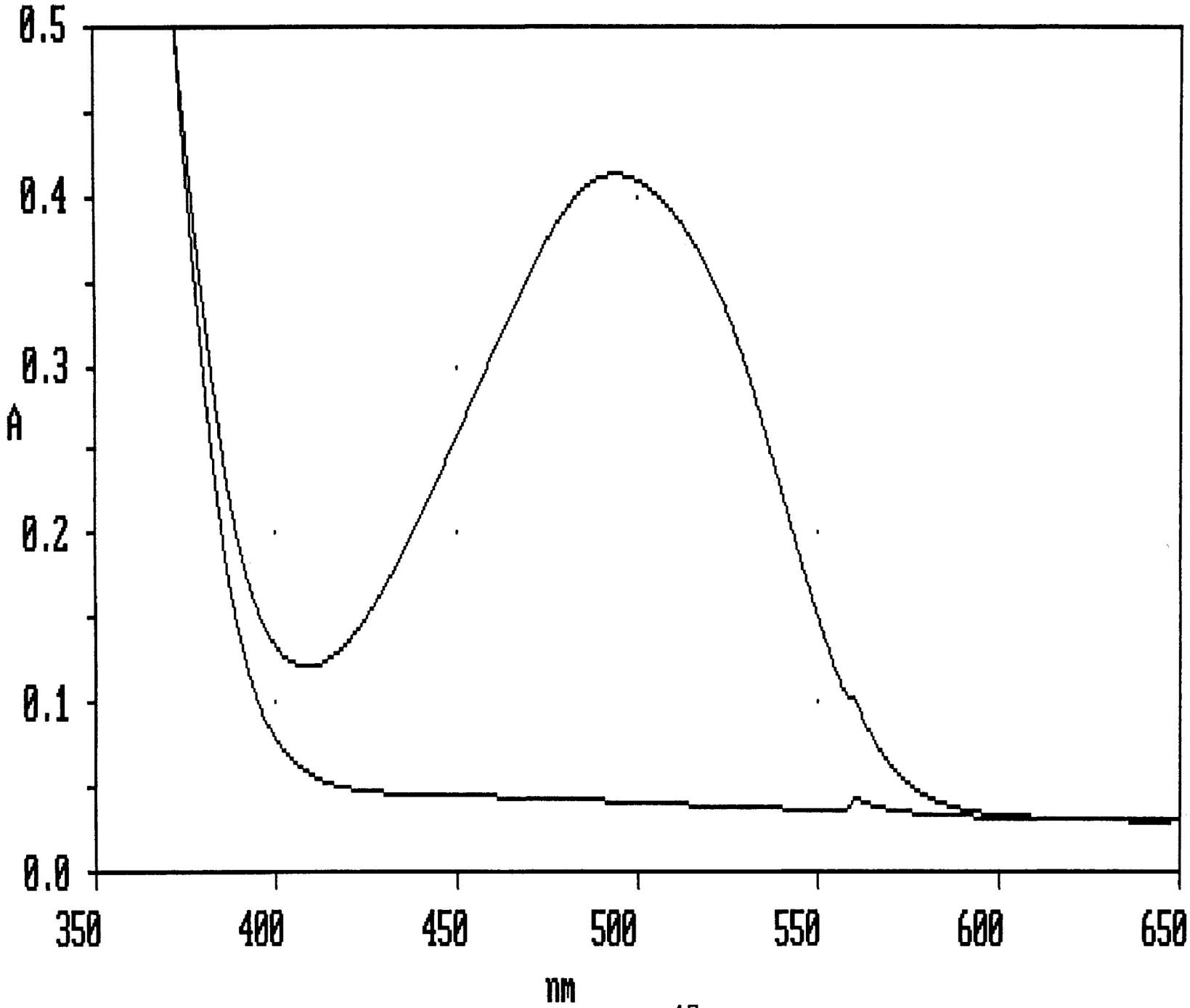

B Photoisomerization of **Z** → **E** of Aberchrome 540 in Solid Polymer Matrices

Table 3.2 lists a set of values of calculated rate constants, k_{1B} and k_{2B}'s, which are used in the kinetic model I(the details are on page 87) to simulate a good fit to the experimental data. The experimental error in the rate constants, k_{1B} is *ca.* 9-10%. The apparent overall(thermal) activation energies for **Z** → **E** are presented in Table 3.3.

Table 3.2 Comparison of calculated apparent rate constants, k_{1B}(calc.) for photoisomerization reaction, **Z** → **E** of Aberchrome 540 in a set of polymer matrices at various temperatures(from Model I).

Temp. (K)	Polymer matrix	Theoretical values		Experi-mental values
		k_{1B}(calc.) (10^{-2} s^{-1})	k_{2B}(calc.) (10^{-2} s^{-1})	k_{2B}(expt.) (10^{-2} s^{-1})
303	PS	2.9	1.5	1.4
	PTBS	9.2	1.7	1.8
	PNBMA	4.7	1.7	1.6
	PVAC	4.9	1.3	1.2

Table 3.2 continued

Temp. (K)	Polymer matrix	Theoretical values		Experi-mental values
		k_{1B}(calc.) (10^{-2} s^{-1})	k_{2B}(calc.) (10^{-2} s^{-1})	k_{2B}(expt.) (10^{-2} s^{-1})
308	PS	3.1	1.5	1.5
	PTBS	9.2	1.8	2.0
	PNBMA	4.7	1.7	1.9
	PVAC	5.0	1.3	1.2
313	PS	5.3	1.6	1.2
	PTBS	9.2	1.9	1.8
	PNBMA	5.5	1.7	1.8
	PVAC	5.7	1.4	1.3
318	PS	5.4	1.6	1.3
	PTBS	9.2	1.9	1.9
	PNBMA	5.6	1.7	1.6
	PVAC	5.7	1.4	1.3

Table 3.2 continued

Temp. (K)	Polymer matrix	Theoretical values		Experi-mental value
		k_{1B}(calc.) (10^{-2} s^{-1})	k_{2B}(calc.) (10^{-2} s^{-1})	k_{2B}(expt.) (10^{-2} s^{-1})
323	PS	5.4	1.6	1.7
	PTBS	9.3	1.9	1.6
	PNBMA	5.6	1.7	1.6
	PVAC	5.7	1.5	1.6
328	PS	5.5	1.6	1.4
	PTBS	9.3	1.9	1.5
	PNBMA	5.7	1.8	1.6
	PVAC	5.8	1.6	1.5
333	PS	5.6	1.6	1.6
	PTBS	9.3	2.0	1.7
	PNBMA	5.7	1.8	1.8
	PVAC	5.8	1.8	1.0

Table 3.2 continued

Temp. (K)	Polymer matrix	Theoretical values		Experi-mental values
		k_{1B}(calc.) (10^{-2} s^{-1})	k_{2B}(calc.) (10^{-2} s^{-1})	k_{2B}(expt.) (10^{-2} s^{-1})
338	PS	5.7	1.8	1.2
	PTBS	9.3	2.2	2.1
	PNBMA	5.8	1.8	1.2
	PVAC	5.8	2.9	2.9

Note that the k_{2B} values used in the calculations, k_{2B}(calc.), are compared with those previously obtained from experiments, k_{2B}(expt.), for the reaction **E** → **C**[46].

Table 3.3 Apparent overall(thermal) activation energies(E_a) related to the calculated k_{1B} at various temperatures(from Model I) for the photoisomerization reaction **Z** → **E** of Aberchrome 540 in various polymer matrices

Polymer matrix	E_a (kJ mol^{-1})
PS	16 ± 3
PTBS	0.38 ± 0.03
PNBMA	5.3 ± 0.7
PVAC	4.1 ± 0.6

i) Absorbance Ratio, A_t/A_∞ Plot

Figure 3.19 presents a sample plot of absorbance ratio, A_t/A_∞ of the red **C** form against time(min) for PVAC at 308 K. A_t and A_∞ reflect the absorbance of **C** form at any given time, t and at a sufficiently long irradiation time, t(∞) approaching the maximum conversion respectively.

Figure 3.19 Plot of A_t/A_∞ of red Aberchrome 540(**c** form) against time(min) at 308 K in PVAC

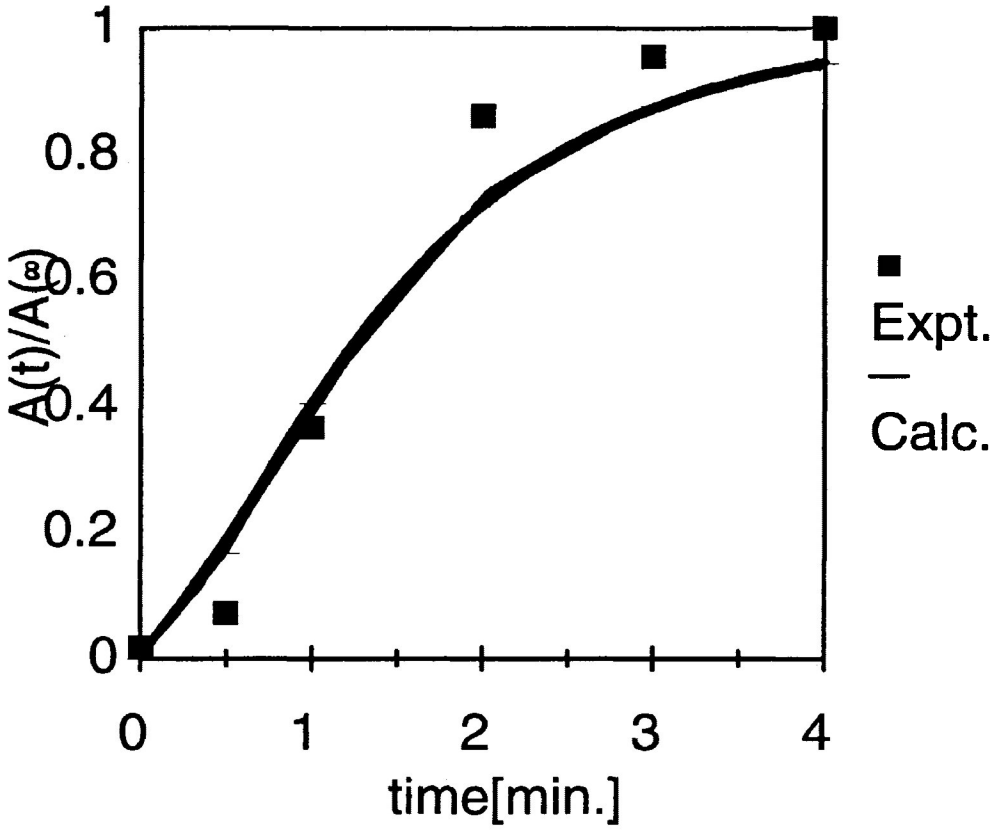

The experimental result(denoted by solid squares) is shown in comparison with the calculated result from Model I(denoted by a solid line), with k_{1B}=5.0 x 10^{-2} s^{-1} and k_{2B} = 1.3 x 10^{-2} s^{-1}.

ii) Graph of a Normalized Ratio, C/Z_0

Figure 3.20 is the fitting of the biphotonic model to the interpolated experimental data at a low conversion factor for PVAC at 308 K. Note that it gives a plot of normalized ratio, C/Z_0 against time(s) in PVAC at 308 K. C is the product formed at any given time, t and Z_0 is the initial concentration of **Z** form.

Figure 3.20 Plot of normalized ratio, C/Z_0, of interpolated experimental result against time(s) for photoisomerization **Z** → **E** at 308 K in PVAC.

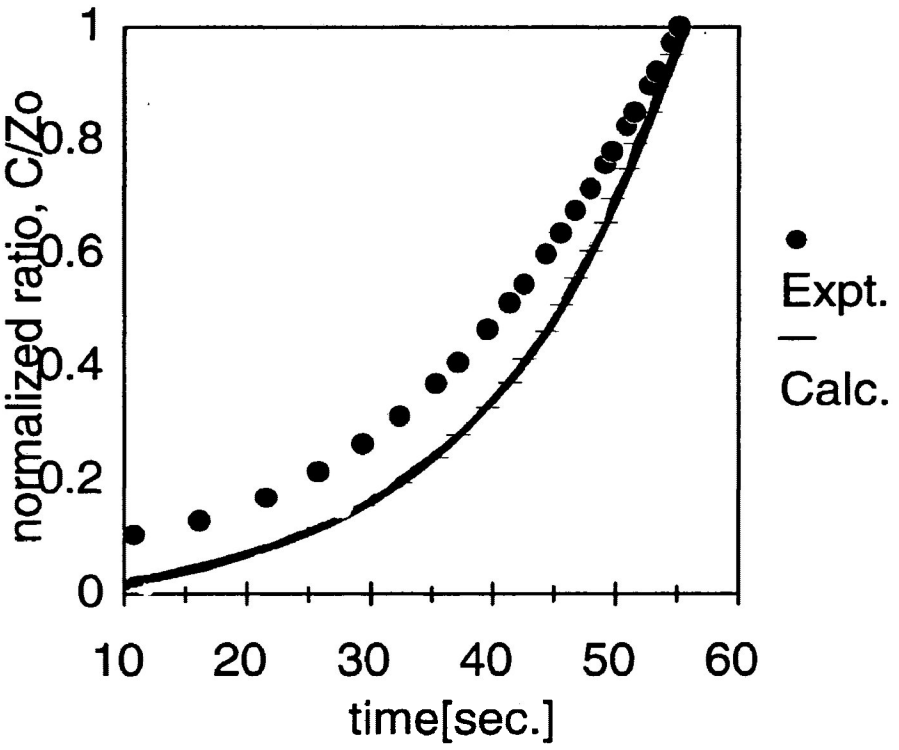

By way of comparison with the experimental result(denoted by circles), the calculated result(denoted by a solid line) is shown. The calculated result is obtained at a low conversion factor with the following parameters:

ϵ_1=8200, ϵ_2=6100, k_{1B} = 5.0 x 10^{-2} s^{-1} and k_{2B} = 1.3 x 10^{-2} s^{-1}.

iii) Plot of a Calculated Ratio, C/Z_0

Figure 3.21 shows the normalized ratio, C/Z_0 against time(s) for PVAC at 308 K under various conditions:

(i) $\epsilon_1(1000) \ll \epsilon_2(6100)$;

(ii) $\epsilon_1(8200) \gg \epsilon_2(1000)$; and

(iii) $\epsilon_1(8200)$ and $\epsilon_2(6100)$.

ϵ_1 and ϵ_2 are the molar absorptivities(unit = $dm^3mol^{-1}cm^{-1}$) of **Z** and **E** forms respectively.

Figure 3.21 Plot of calculated normalized ratio, C/Z_0 against time(s) for the photoinduced reaction of **Z** → **E** → **C** of the dye in PVAC at 308 K

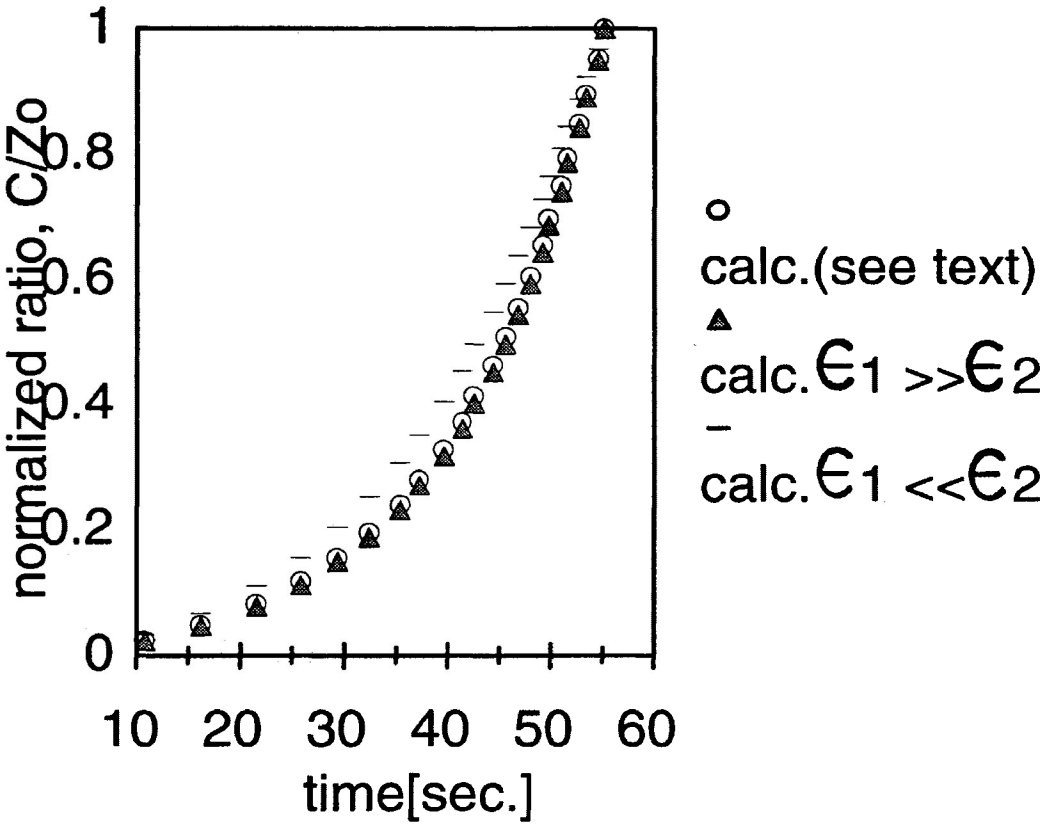

The same k_{1B} = 5.0 x 10^{-2} s^{-1} and k_{2B} = 1.3 x 10^{-2} s^{-1} are used under various conditions:

(i) $\epsilon_1(1000) \ll \epsilon_2(6100)$ (denoted by dashed lines);

(ii) $\epsilon_1(8200) \gg \epsilon_2(1000)$ (denoted by triangles);

(iii) ϵ_1=8200 and ϵ_2=6100 (denoted by circles).

C Photobleaching of **C** → **E** of Aberchrome 540 in Solid Polymer Matrices at Low Temperatures

i) Absolute Output Voltage Plot

In the photocolouration process discussed earlier, i.e. **E** → **C**, the product(red **C** form)is followed at various times. However, in the reverse process, the photobleaching, i.e. **C** → **E**, the reactant(**C** form) remaining at any given time,t is determined. The kinetic equation for the photobleaching is

$$\ln(V_t - V_\infty) = -kt \pm \ln(V_0 - V_\infty) \text{---(10)},$$

where V_0 , V_t, and V_∞ are the absolute output voltage proportional to the red dye(**C** form) at time zero, at any time,t, and at a sufficiently long time approaching maximum conversion(to **E** form) respectively.

Table 3.4 represents the rate constant values(in seconds) for k_{2C}(at a sufficiently long time) at 83-303 K for the dye reaction in PS and PC. The experimental error in the rate constant values is *ca.*7-9%.

Figures 3.22-3.49 are plots of $\ln(V_t - V_\infty)$ of Aberchrome 540 in red **C** form against time(min) in PS and PC respectively, at specified temperatures. It is worth mentioning that the data shown in each curve as in Figures 3.22-3.49 are the results of three trials. Figures 3.50-3.51 represent the Arrhenius plots of the photobleaching of

Aberchrome 540(**C** form) in PS and PC respectively. As seen in the photocolouration of Aberchrome 540(**E** form) in polymer matrices previously[46], whereby two distinct slopes are observed, the same feature is clearly observed during the photobleaching process in the current experiment, which is also done in the polymer media. However, the reasons leading to the observed results are not the same. This allows for the extraction of the two apparent first-order rate constants: k_{1C}(from the first line of the plot) and k_{2C}(from the second line of the plot). In thicker sample mixtures(mixtures of dye and polymer in solvent for casting sample films), k_{1C} is derived from the reaction at a shorter time about 1-2 minutes after irradiation times for PS and 0.1-0.2 minutes for PC, followed by the reaction toward the end of the irradiation times(from which k_{2C} is derived). In almost all the cases, the line providing the first slope of each plot covers less data points than the second line. The short initial time may be related to some unknown induction factor. As a result, the data show somewhat less significant changes to be accounted for. For this reason, the rate constants k_{1C} are less meaningful and are not shown. Only the rate constants k_{2C} are presented.

Table 3.4 Tabulated data for rate constants k_{2C} for the photobleaching reaction of Aberchrome 540(C form) in PS and PC

Temp. studied(K)	Poly(styrene)	Poly(carbonate)
	Rate constant, k_{2C} (10^{-2} s^{-1})	Rate constant, k_{2C} (10^{-2} s^{-1})
83	3.8	5.6
103	4.7	7.5
123	6.0	7.7
143	7.6	9.1
163	4.3	6.8
183	9.6	6.8
203	12.3	9.0

Table 3.4 continued

Temp. studied(K)	Poly(styrene)	Poly(carbonate)
	Rate constant, k_{2c} (10^{-2} s^{-1})	Rate constant, k_{2c} (10^{-2} s^{-1})
223	3.1	9.3
243	15.7	4.2
263	7.2	9.0
283	3.6	11.2
303	4.2	8.0

Figure 3.22 Plot of $\ln(V_t - V_\infty)$ of red Aberchrome 540(C form) against time(min) at 83 K in PS

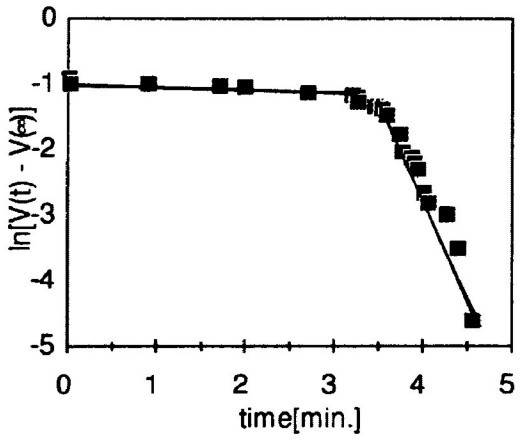

Figure 3.23 Plot of $\ln(V_t - V_\infty)$ of red Aberchrome 540(C form) against time(min) at 103 K in PS

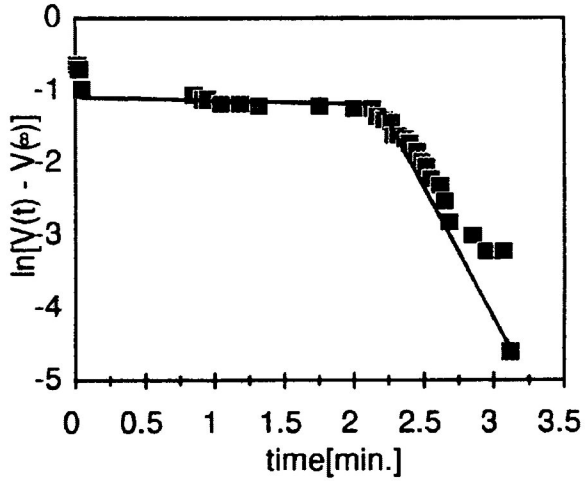

Figure 3.24 Plot of $\ln(V_t - V_\infty)$ of red Aberchrome 540(C form) against time(min) at 123 K in PS

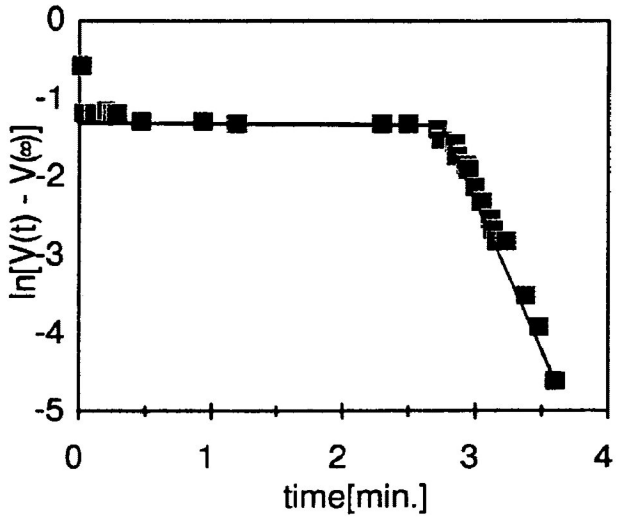

Figure 3.25 Plot of $\ln(V_t - V_\infty)$ of red Aberchrome 540(C form) against time(min) at 143 K in PS

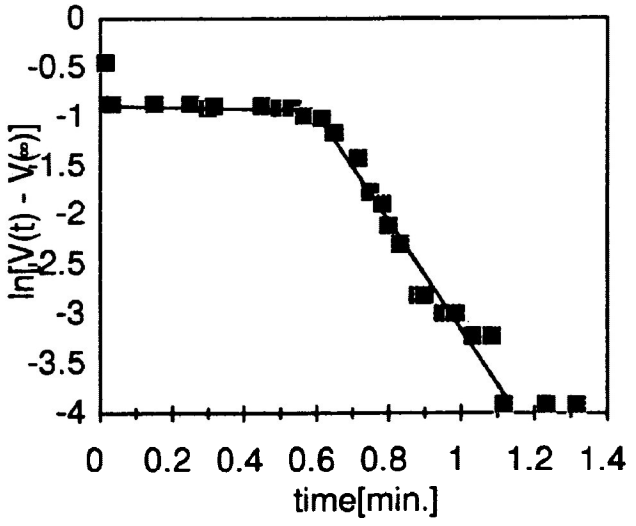

Figure 3.26 Plot of $\ln(V_t - V_\infty)$ of red Aberchrome 540(C form) against time(min) at 163 K in PS

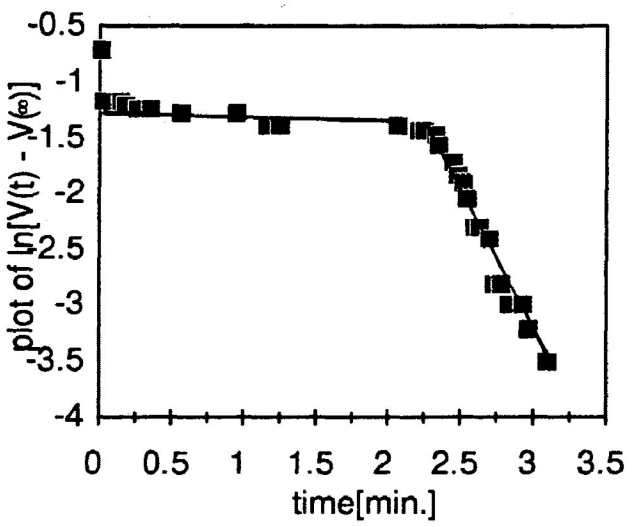

Figure 3.27 Plot of $\ln(V_t - V_\infty)$ of red Aberchrome 540(C form) against time(min) at 183 K in PS

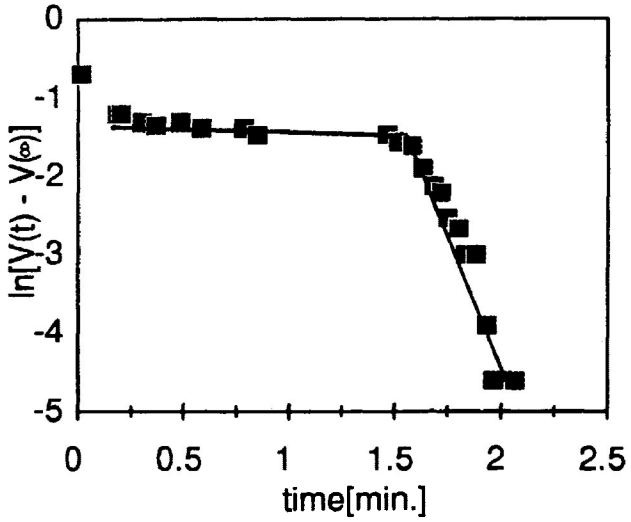

Figure 3.28 Plot of $\ln(V_t - V_\infty)$ of red Aberchrome 540(**C** form) against time(min) at 203 K in PS(in thicker sample mixtures)

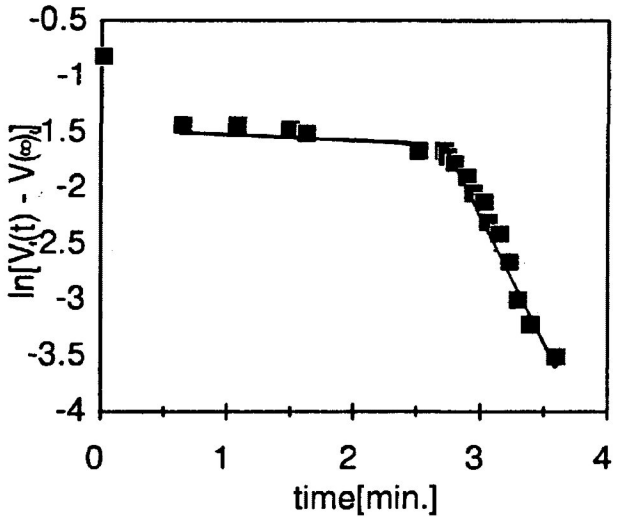

Figure 3.29 Plot of $\ln(V_t - V_\infty)$ of red Aberchrome 540(**C** form) against time(min) at 203 K in PS(in thinner sample mixtures)

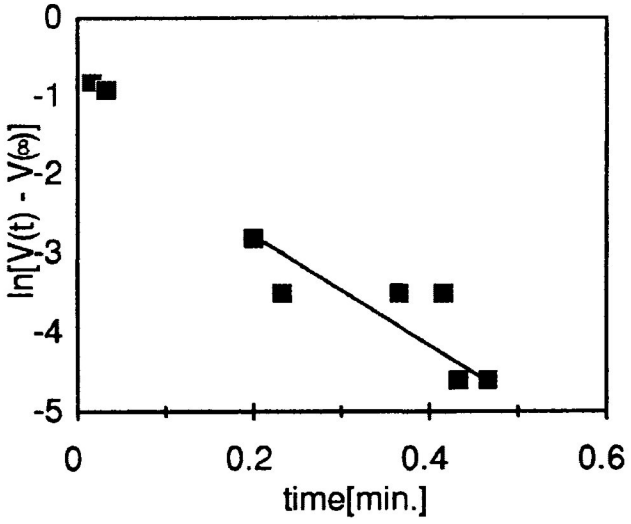

Figure 3.30 Plot of $\ln(V_t - V_\infty)$ of red Aberchrome 540(C form) against time(min) at 223 K in PS(in thicker sample mixtures)

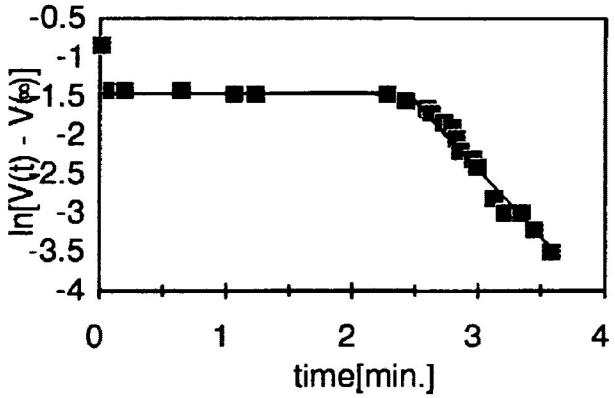

Figure 3.31 Plot of $\ln(V_t - V_\infty)$ of red Aberchrome 540(C form) against time(min) at 223 K in PS(in thinner sample mixtures)

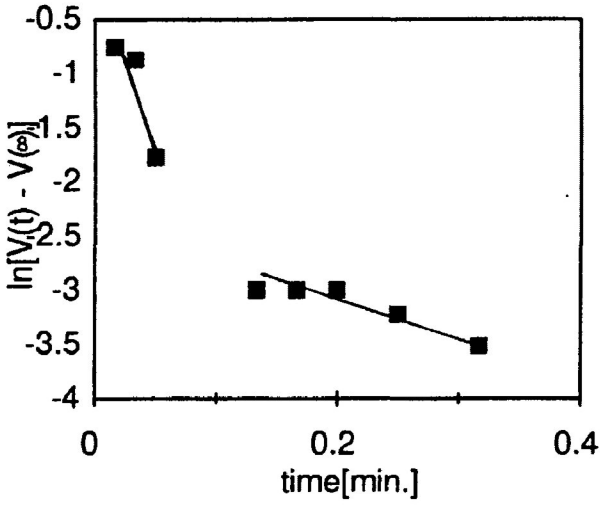

Figure 3.32 Plot of $\ln(V_t - V_\infty)$ of red Aberchrome 540(**C** form) against time(min) at 243 K in PS(in thicker sample mixtures)

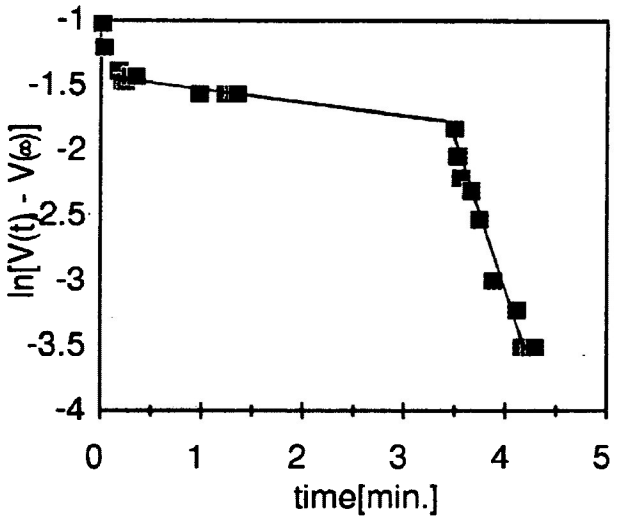

Figure 3.33 Plot of $\ln(V_t - V_\infty)$ of red Aberchrome 540(**C** form) against time(min) at 243 K in PS(in thinner sample mixtures)

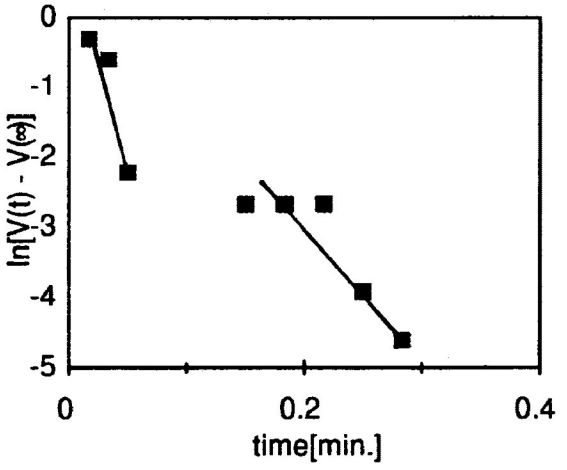

Figure 3.34 Plot of $\ln(V_t - V_\infty)$ of red Aberchrome 540(**c** form) against time(min) at 263 K in PS(in thicker sample mixtures)

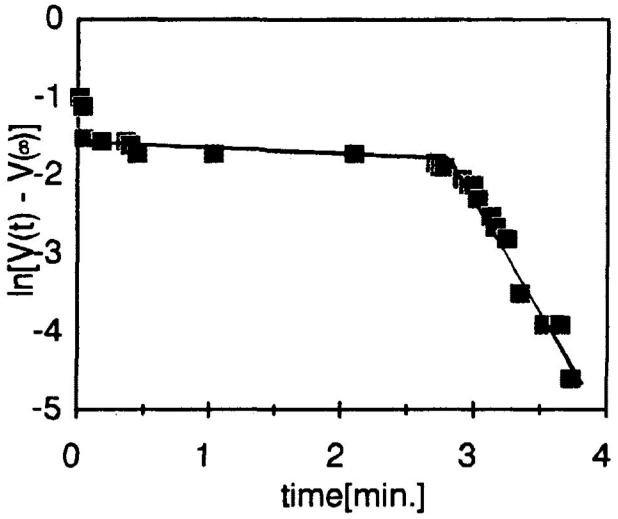

Figure 3.35 Plot of $\ln(V_t - V_\infty)$ of red Aberchrome 540(**c** form) against time(min) at 263 K in PS(in thinner sample mixtures)

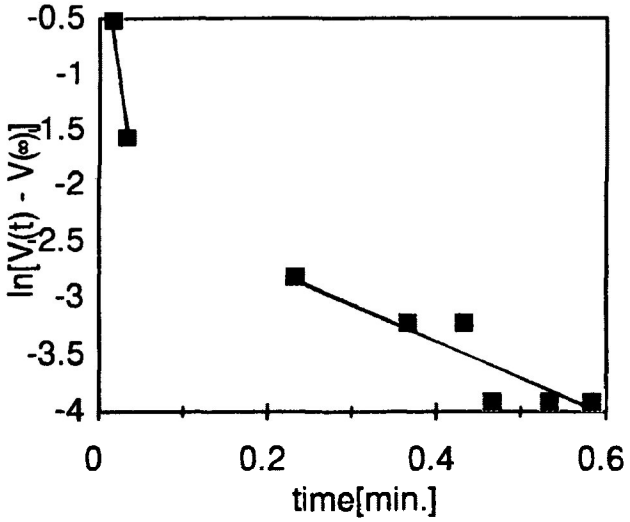

Figure 3.36 Plot of $\ln(V_t - V_\infty)$ of red Aberchrome 540(**C** form) against time(min) at 283 K in PS

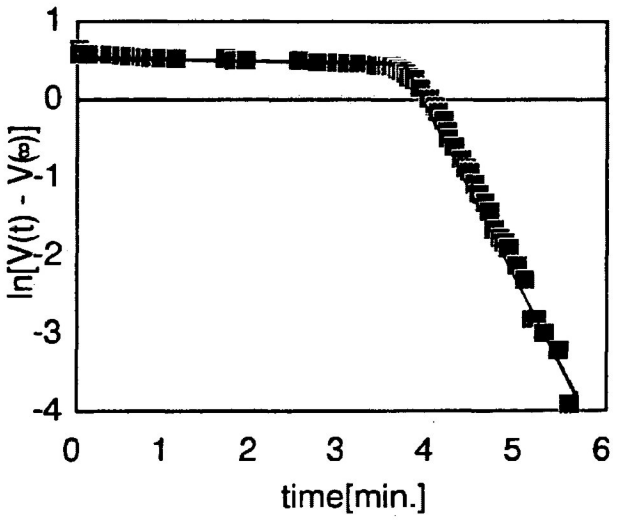

Figure 3.37 Plot of $\ln(V_t - V_\infty)$ of red Aberchrome 540(**C** form) against time(min) at 303 K in PS

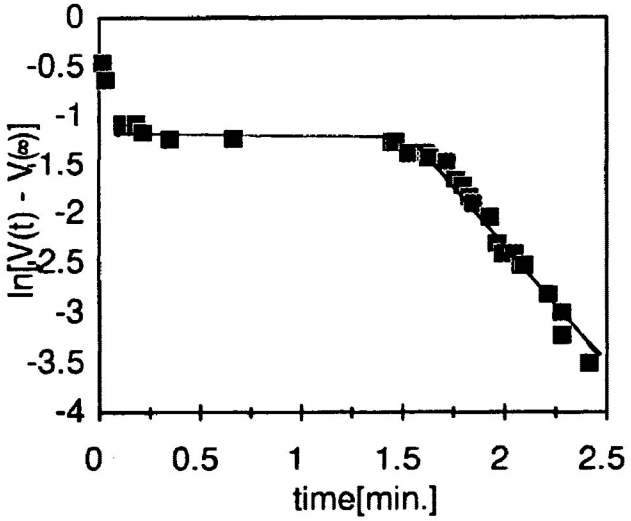

Figure 3.38 Plot of $\ln(V_t - V_\infty)$ of red Aberchrome 540(**C** form) against time(min) at 83 K in PC

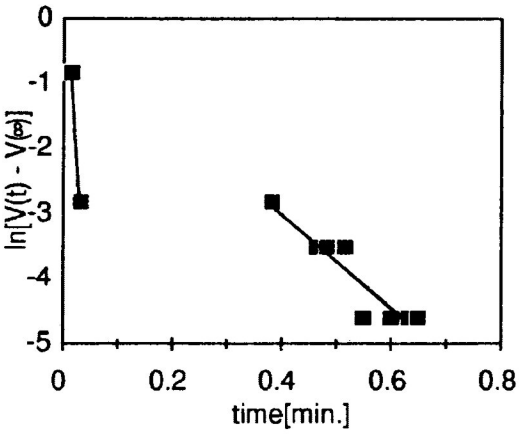

Figure 3.39 Plot of $\ln(V_t - V_\infty)$ of red Aberchrome 540(**C** form) against time(min) at 103 K in PC

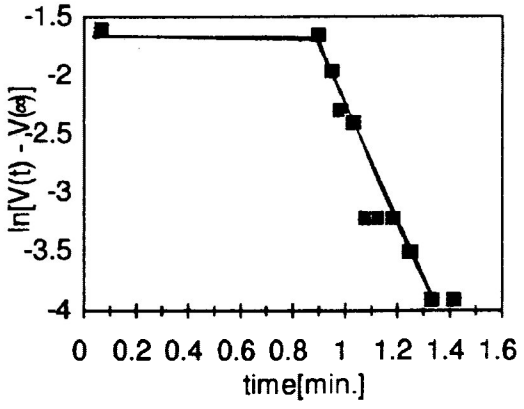

Figure 3.40 Plot of $\ln(V_t - V_\infty)$ of red Aberchrome 540(**C** form) against time(min) at 123 K in PC

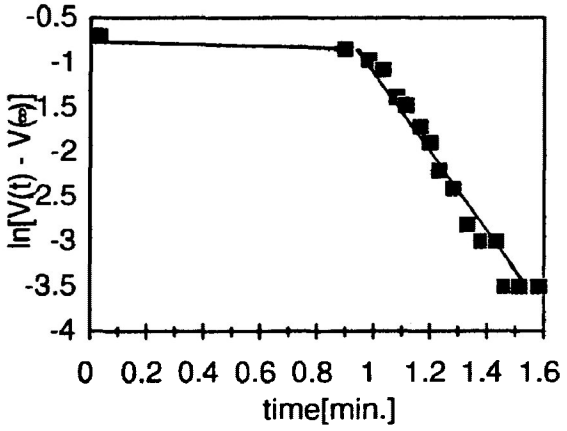

Figure 3.41 Plot of $\ln(V_t - V_\infty)$ of red Aberchrome 540(**C** form) against time(min) at 143 K in PC

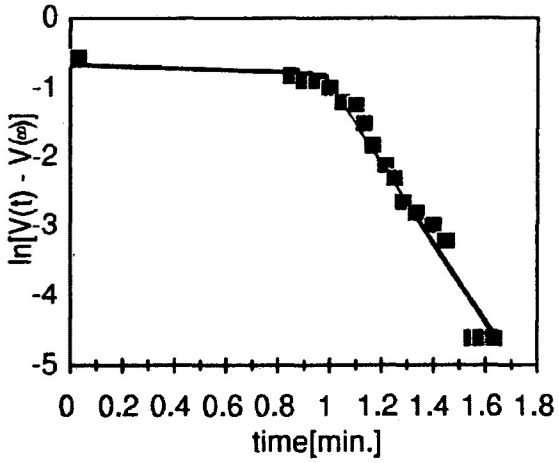

Figure 3.42 Plot of $\ln(V_t - V_\infty)$ of red Aberchrome 540(C form) against time(min) at 163 K in PC

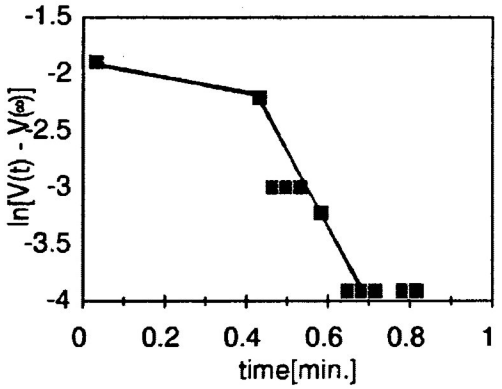

Figure 3.43 Plot of $\ln(V_t - V_\infty)$ of red Aberchrome 540(C form) against time(min) at 183 K in PC

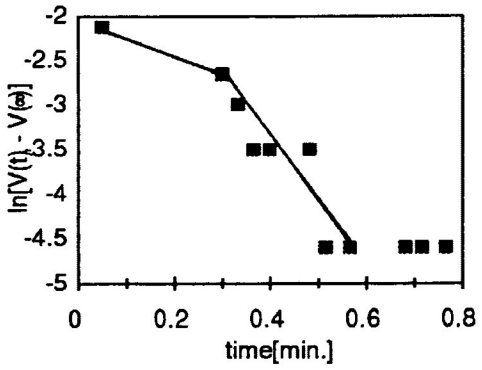

Figure 3.44 Plot of $\ln(V_t - V_\infty)$ of red Aberchrome 540(**C** form) against time(min) at 203 K in PC

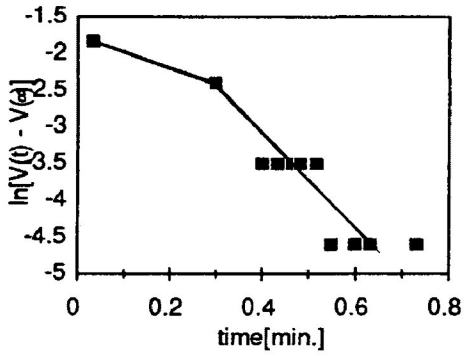

Figure 3.45 Plot of $\ln(V_t - V_\infty)$ of red Aberchrome 540(**C** form) against time(min) at 223 K in PC

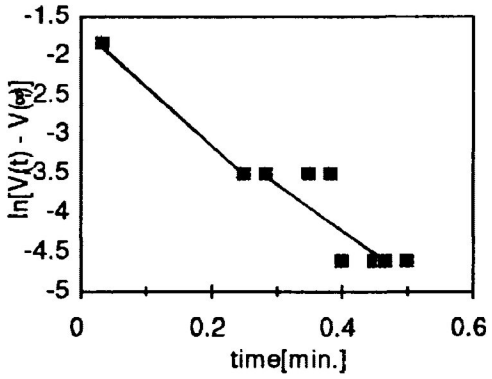

Figure 3.46 Plot of $\ln(V_t - V_\infty)$ of red Aberchrome 540(**C** form) against time(min) at 243 K in PC(in thicker sample mixtures)

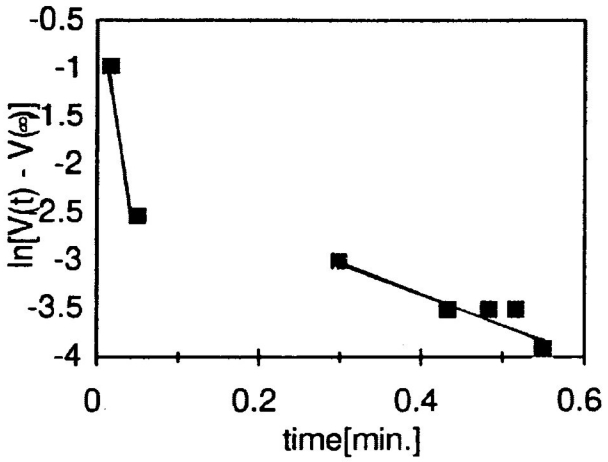

Figure 3.47 Plot of $\ln(V_t - V_\infty)$ of red Aberchrome 540(**C** form) against time(min) at 263 K in PC(in thicker sample mixtures)

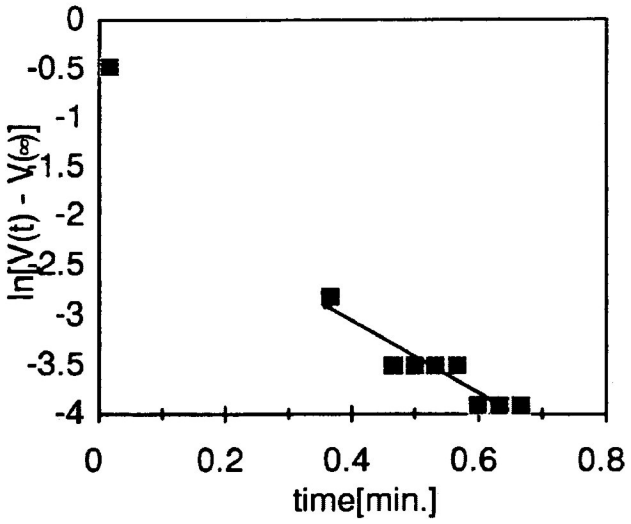

Figure 3.48 Plot of $\ln(V_t - V_\infty)$ of red Aberchrome 540(**c** form) against time(min) at 283 K in PC

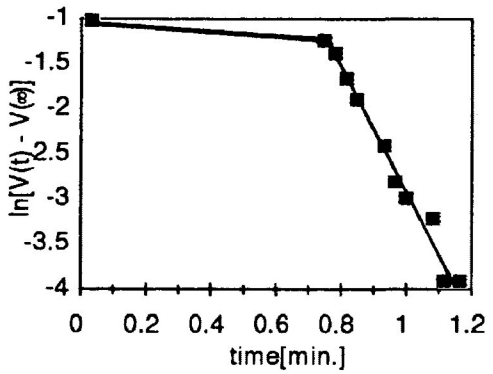

Figure 3.49 Plot of $\ln(V_t - V_\infty)$ of red Aberchrome 540(**c** form) against time(min) at 303 K in PC

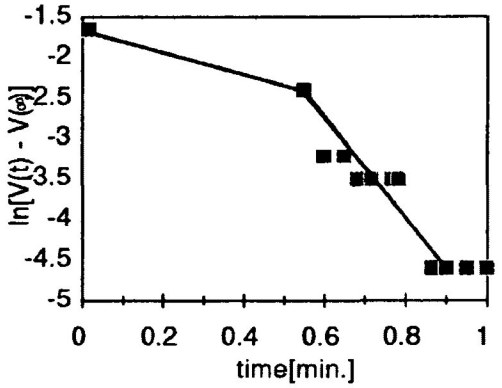

ii) Arrhenius plot

By using equation (8), the apparent overall(thermal) activation energy is determined. Table 3.5 shows the comparison of the apparent overall(thermal) activation energies, E_a obtained from k_{2c} as a function of temperature in PS and PC. It is important to note that the E_a's for PS and PC in Table 3.5 are calculated from the average of both slopes(as seen in Figures 3.50-3.51) for each set.

Figures 3.50 and 3.51 are the Arrhenius plots of the photobleaching of Aberchrome 540(**c** form) in PS and PC respectively.

Table 3.5 Apparent overall(thermal) activation energies correspond to the rate constants k_{2c} for the photobleaching reaction of Aberchrome 540(**c** form) in PS and PC

Polymer	Activation energy, E_a (kJ mol^{-1})
PS	1.5 ± 0.1
PC	0.6 ± 0.1

Figure 3.50 Arrhenius plot of the photobleaching of Aberchrome 540(**C** form) in PS

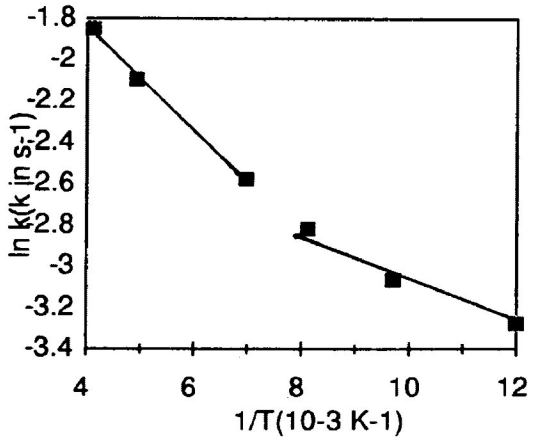

Figure 3.51 Arrhenius plot of the photobleaching of Aberchrome 540(**C** form) in PC

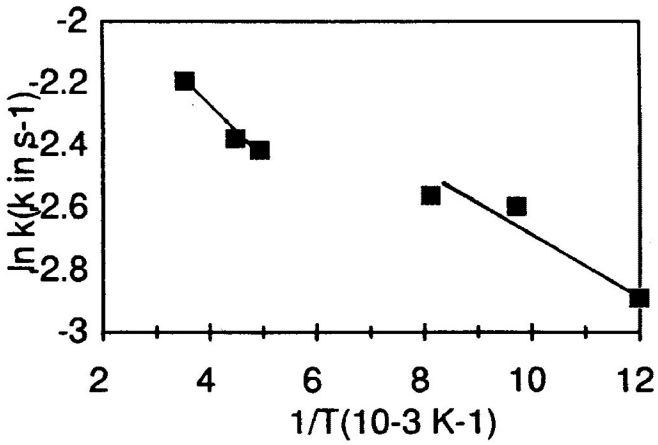

4 DISCUSSION

4.1 Photo-Induced Reactions of A Dye in Polymer Matrices and in Solvents

4.1.1 Kinetic Analysis

A Photocolouration of **E** → **C** of Aberchrome 540 in Solvents

In an attempt to investigate the with and without the interfering effect due to limited mobility of solid polymer media, the photocolouration of the amber dye(**E** → **C**) in a number of solvents with varying polarity has been conducted in the present work. The following aspects are considered to play important roles in the photocolouration of the amber **E** form of Aberchrome 540 in solvents and in polymer matrices:

i)Conformation factor against matrix effect

ii)Rate of dye reaction.

i) Conformation Factor against Matrix Effect

A previous study[46] of the photocolouration **E** → **C** in polymer matrices has shown two distinct lines of each of the first-order plots. It is suggested that the chemical reaction kinetics of the photocolouration from ring-opened(**E** form) to the ring-closure(**C** form) is not caused by factor

i) the solid matrix that restricts/controls the movement of the dye molecules during the photoisomerization; but by factor

ii) the possible existence of two major conformers of the ring-opened dye molecules trapped in the solid matrix.

Factor (i) is suggested to be the cause of deviation from the

first-order plot of the thermal bleaching of merocyanine to spiropyran[34,36] and the cis-trans photoisomerization of azobenzene[94-95], 1,1'-azonapthalene[51,95], and 9,9'-azophenanthrene[52]. On the contrary, such deviation from linearity is not observed for the previous reaction[46] and therefore factor (i) is unlikely to dominate here.

If factor (ii) is the dominating factor, then two possibilities for the photoinduced reaction exist:

(iia)one occurs through a typical parallel first-order reaction described below:

$$E' \xrightarrow{k_a} C \text{---(11)}$$

$$E'' \xrightarrow{k_b} C \text{---(12)}$$

Note that both conformers **E'** and **E"** react to form **C** with the corresponding rate constants k_a and k_b. Then rate equations are as follow: $E' = E_0' \exp(-k_a t)$, $E'' = E_0'' \exp(-k_b t)$, and $C_\infty = E_0' + E_0''$, where C_∞ = total concentration of the red **C** form, E_0' and E_0'' are the original concentrations of E' and E" respectively. Thus, at any time,t, the concentration of the red **C** form, $C_t = C_\infty - E' - E''$

$$= (E_0' + E_0'') - E' - E''$$

$$= C_\infty - E_0' \exp(-k_a t) - E_0'' \exp(-k_b t) \quad \text{---(13)}.$$

Equation (13) leads to composite first-order kinetics and results in a deviation from linearity in the case of $k_a \neq k_b$. (iib)one occurs through a typical consecutive first-order reaction, i.e. the reaction shows two first-order processes, one after another, which is the case for the previous[46] photoinduced reaction, suggesting the possible existence of two major conformers of E form trapped in solid matrix. The observation is partially supported by the ability[80] of the dye molecule to undergo rotation around the C-C single bond, connecting the C-3 of the furan ring to the α-C of the ethylidene as seen in Scheme 1, generating various possible conformations. Since the same photoinduced reaction in each of the present solvent gives only one straight line, which is observed in the first-order plots in Figures 3.1-3.16, the present reaction kinetics in solvents partially support the existence of two major conformers of the dye molecules in solid polymer matrix.

To elaborate further, several arguments are presented below.

The following factors may affect the reaction kinetics: the solvent polarity effect, the solvent viscosity effect, reaction temperature, and the intermolecular hydrogen bond formation between the dye and the solvent molecules.

I.R. analyses[11] reveal significant hydrogen bond interaction between red dye(**C** form) molecules of Aberchrome 540 and a number of solvents[96]. The previous[10-11] photobleaching **C** → **E** reactions(give only one straight line), which involve only one isomeric reactant of the **C** form, have indicated that the differences in the dye sites(considering the dipolar interactions between the **C** form and the medium) do not cause the deviation from linearity of the first-order plot. Deviation from linearity is also found with the photocolouration of ring-opened(**E** form) to the ring-closure(**C** form)in polymer matrices[46]. A similar explanation may be extended to explain the present study since the size of the amber **E** form is not much different from the red **C** form[46].

Other details supporting the significant role of the conformation factor against the matrix effect for the observed kinetics in the previous study[46] come from the present photocolouration reaction of **E** form in solvents. Information is obtained from the comparison of rate constants of similar dye reactions in PS with the average rate constant values in all liquids used at 303 K. At 303 K, the single rate constant in PS and the average rate constant value in the liquids are 1.4×10^{-2} sec^{-1}[46] and 0.96×10^{-2} sec^{-1} respectively. There is little difference between those rate values. Nonetheless, such a phenomenon is commonly reported in other systems[77,97]. Perhaps there is adequate free volume available at the dye site for the cyclization to the ring-

closure red **C** form. Otherwise, a similar situation is observed involving deviation from linearity such as in the thermal cis-trans isomerization of azobenzene in polymer[94-95]. Also note that there is only one isomeric cis- or trans-form of azobenzene presents.

ii) Effects on the Rate Constants of Dye Reaction

As mentioned briefly earlier, there are several common factors that may affect the rate of a non-ionic chemical reaction, which is applicable to the present work. They are: (a) the effect of medium polarity on rate constants, k_{1A}, (b) the effect of reaction temperature on k_{1A}, (c) the viscosity effect on k_{1A}, and (d) the hydrogen bonding effect on k_{1A}.

(a) The effect of medium polarity on rate constants, k_{1A}.

Quite recently, several studies[98-101] have investigated the effect of solvent polarity on the rate of a photoisomerization reaction. Inspection of Table 3.1 for the k_{1A} values of the photocolouration of the **E** form dye shows that there is only a small difference observed in k_{1A} values. This general trend, which is observed at all temperatures studied, reveals only small differences in k_{1A} values (from 0.07 to 1.0) for non-dipolar solvents (cyclohexane and n-heptane), a weakly dipolar solvent (toluene), and for moderately dipolar solvents (ethyl acetate, chloroform, t-pentanol, acetonitrile,

and ethanol). The small differences are within the experimental errors. From 298-303 K, for example, k_{1A} of the dye reaction in cycohexane increases by 0.1. The same reactions, from 298-303 K, in t-pentanol and ethanol differ by 0.05 and 0.04 respectively. For n-heptane, toluene, ethyl acetate and chloroform, however, the rate constants of the dye reaction decrease by 0.05, 0.07, 0.02, and 1.0 respectively. From 303-308 K, again there are only small differences in the k_{1A} observed. In ethanol, k_{1A} differs by 0.4, while no difference is observed in k_{1A} for n-heptane. On the other hand, k_{1A} values in cyclohexane, toluene, ethyl acetate, chloroform, t-pentanol, and acetonitrile decrease by 0.07, 0.07, 0.1, 0.3, 0.02, and 0.01 respectively. The small differences among the rate constants for the reaction in various solvents indicate that the rates of the photocolouration of **E** form are unaffected by solvent polarity.

(b) <u>The effect of reaction temperature on k_{1A}</u>.

Due to the small differences in rate constants, k_{1A} at various temperatures for a given solvent, as alluded to in (a), none of the overall apparent(thermal) activation energies, E_a for the dye reaction are calculated. The thermal activation energies are very small.

(c) <u>The viscosity effect on k_{1A}</u>.

If the viscosity factor causes the decrease in

reaction rate, then t-pentanol(η=3.706 mPas) and ethanol(η=1.074 mPas) due to their relatively larger viscosities should be more affected by it than cyclohexane(η = 0.894 mPas), n-heptane(η = 0.386 mPas), toluene(η = 0.568 mPas), ethyl acetate(η = 0.423 mPas), chloroform(η = 0.542 mPas), and acetonitrile(η = 0.345 mPas). Such a phenomenon is not observed here. Especially for associated liquids such as an ethanol and a weakly associated liquid(chloroform), other factor such as the presence of intermolecular hydrogen bonding between the dye and the solvent molecules may play an important role. This is further discussed in (d).

(d) The hydrogen bonding effect on k_{1A}.

A study[102] has shown that some intermolecular interactions occur between a benzene molecule and a water molecule. If such weak interactions can occur between the benzene(which is non-polar)and water molecules, then the same weak intermolecular interactions are even more likely to occur between polar molecules in both dye and liquid media such as ethyl acetate, chloroform, t-pentanol, and ethanol. The rate constants k_{1A} are observed to be greater in ethanol and chloroform, at all temperatures, than in other polar solvents such as ethyl acetate, t-pentanol, and acetonitrile. The plausible existence of the weak intermolecular H-bonding is supported by a previous I. R. study[96] from this laboratory. The coupling frequencies belonging to the carbonyl

groups[103-104] of the succinic anhydride moiety of the red dye in a non-dipolar and non-associated n-heptane, appears at 1817 and 1769 cm^{-1}. These corresponding frequencies are shifted to 1814 and 1764 cm^{-1} in an associated liquid such as 1-pentanol. Such a shift to a lower wave number(relative to n-heptane) in a dipolar protic solvent indicates the ability of the solvent to form hydrogen bonds with the red dye. The hydrogen bonds are formed between the O atoms of the carbonyl groups with the H atoms of the -OH groups(of alcohols) and could better stabilize the red **C** form than the **E** form. While the exact reasons leading to the higher k_{1A} in ethanol and in chloroform than in other solvents are not known, it is plausible that stabilization of the product(**C** form) by associated solvents may lower the overall activation energies. Hence, the observed rate constants are obtained.

iii) Possibility of Dye Molecules Interactions

It is worth mentioning that the possibility of interactions between dye molecules, which may complicate the kinetic results in the present work, has been further investigated by increasing the dye concentration by a factor of 1.5. There is no significant differences in the values of k_{1A}, within the experimental errors. Therefore, the possibility of dye-dye interaction in the current work may be neglected.

B Photoisomerization of **Z** → **E** of Aberchrome 540 in Solid Polymer Matrices

This area of the current work can be treated as a complement to the above study. The main topics of the research comprise the general aspects of the study, a typical kinetic model(Model I) for the two consecutive first-order reactions, a biphotonic model(Model II), and finally, on the calculated results from Model I.

i) General Aspects

A sample plot of the product(**C** form) normalized against the maximum conversion expressed as A_t/A_∞ versus time(min) is presented in Figure 3.19. A typical characteristic of the plot for the photoinduced reaction in polymers is the fact that the plot shows a sigmoidal curve, which typifies a curve of the final product for the first-order consecutive reactions. Such a feature is observed in all polymer matrices investigated. It should be noted that **E** form is further isomerized to the **C** form. The absorption spectra of **Z** and **E** forms are similar. Thus the rate constant for the photoisomerization **Z** → **E** cannot be directly determined, so that some consecutive kinetic models are required to treat such limitations.

ii) A Typical Kinetic Model: Model I

The simplest consecutive first-order mechanism is

shown in Scheme 2 below.

Scheme 2 A two consecutive first-order reaction

$$\mathbf{Z} \xrightarrow{k_{1B}} \mathbf{E} \xrightarrow{k_{2B}} \mathbf{C}$$

If the initial concentrations of **Z** is Z_0, then the rate equations for the change of the concentrations of **Z**, **E**, and **C** at any given time, t with the corresponding solutions for **Z** and **E** are:

$$\frac{dZ}{dt} = -k_{1B}Z,\ Z = Z_0 e^{-k_{1B}t} \text{---(14)}$$

$$\frac{dE}{dt} = k_{1B}Z - k_{2B}E,\ E = \frac{Z_0 k_{1B}}{k_{2B} - k_{1B}}\left(e^{-k_{1B}t} - e^{-k_{2B}t}\right) \text{---(15)}$$

$$\frac{dC}{dt} = k_{2B}E \text{---(16)}.$$

Note that Z + E + C = Z_0, thus

$$C = Z_0 - Z - E \text{---(17)}.$$

Insertion of the expressions for Z and E into equation (17) leads to

$$C = \frac{Z_0}{k_{2B} - k_{1B}} [k_{2B}(1 - e^{-k_{1B}t}) - k_{1B}(1 - e^{-k_{2B}t})],$$

or

$$\frac{C}{Z_0} = \frac{1}{k_{2B} - k_{1B}} [k_{2B}(1 - e^{-k_{1B}t}) - k_{1B}(1 - e^{-k_{2B}t})].$$

Equivalent expression for the above equation is

$$\frac{A(t)}{A(\infty)} = \frac{1}{k_{2B} - k_{1B}} [k_{2B}(1 - e^{k_{1B}t}) - k_{1B}(1 - e^{-k_{2B}t})] \text{---(18), where}$$

A(t) and A(∞) are the absorbance of **C** form at any given time, t, and at a sufficiently long irradiation time t(∞) for **Z** form to approach the maximum conversion to **C** form respectively.

To obtain a proper fit to the experimental data, results from the theoretical calculation, equation (18) is used to simulate such fittings. The theoretical calculations were done using a computer program, KINFIT[105], by varying k_{1B} and k_{2B} at various times, t, so that the absorbance ratio

$A(t)/A(\infty)$ would give the best fit to the experimental data. In the present work, the theoretical kinetic model seems to fit the corresponding experimental yields reasonably well[105] within the experimental error margin. The kinetic model has its advantages. Only one unknown variable of k_{1B} is involved. The k_{2B} is known from the previous experiment(**E** → **C**)[46]. Hence, the model is less flexible. A typical sample plot of the calculated results is shown in curve of Figure 3.19.

iii) A Biphotonic Model: Model II

As seen in Scheme 2, the two consecutive reactions may also be viewed as a two-photon/biphotonic process. **Z** absorbs the first photon to form **E** with the rate constant k_{1B}, followed by **E**, which absorbs the second photon to yield the final product **C** with the rate constant k_{2B}.

Studies related to such a process include the determination of quantum yields by both the fluorescence method and the absorbance of the reacting system[106], a semiclassical treatment of a quantum mechanical model[107], and a quantum electrodynamic model[108]. For the present work, another type of theoretical kinetic model(Appendix C) is adopted. The model presents several difficulties, which are due to the simplifying assumptions, since there is no analytic solution to the approach.

For comparison, both data from the interpolated experimental results and from the theoretical calculations

derived from equation C6(Appendix C) are presented in Figure 3.20. The plot shows the ratio of C/Z_0, which is normalized to 1, against time(sec). The calculation considers a maximum limit of only up to 25% conversion of **z** to **c** form because high conversion would invalidate[105] one of the basic assumptions of this model, as shown in Appendix C. The theoretical calculation requires known k_{2B} values obtained from the previous[46] experimental data(part of a series to this work), the calculated k_{1B} values from Model I, and the known molar absorptivities ϵ_1 and ϵ_2.

Several conclusions can be drawn from the observations at such a low conversion limit. Firstly, the normalized ratio,C/Z_0 yield is somewhat less than the experimental result at a given time as seen in Figure 3.20. The values of k_{1B} and k_{2B} are varied within a reasonable limit with k_{2B}/k_{1B} changes from 0.26 to 0.50 to obtain a better fit for the experimental results. Surprisingly, the results do not show much change. Perhaps the model is insensitive to the parameter k_{1B}, suggesting that there may be enough photons in the system and hence no real competition for the photons for the reaction, although mechanistically(as seen in Scheme 2), the reaction should be biphotonic. Secondly, the biphotonic model(Model II) underestimates the yield. However, Model I slightly overestimates the yield, as seen in Figure 3.20. This may be caused by a slight discrepancy between the experimental and the calculated theoretical results of Model

I. The discrepancy, however, might have been minimized by the inclusion of the biphotonic effect, which tends to underestimate the outcome. It is worth noting that such a discrepancy falls within the present margin of experimental errors[105].

To further examine the biphotonic model, two extreme cases are discussed:

i) $\epsilon_1(1000) \prec\prec \epsilon_2(6100)$ (result appears in Figure 3.21); and

ii) $\epsilon_1(8200) \succ\succ \epsilon_2(1000)$ (result appears in Figure 3.21).

iii) $\epsilon_1(8200)$ and $\epsilon_2(6100)$ (result appears in Figure 3.20) is presented as a comparison. Units of ϵ_1 and ϵ_2 are in $dm^3mol^{-1}cm^{-1}$. All conditions use the same k_{1B} and k_{2B} values used in Figure 3.19, which gives a good fit. The explanations for the above conditions are as follow: The results of condition (i)-(ii), as appear in Figure 3.21, produce almost the same results. However, condition (i), using only the predicted value for ϵ_1 of the present experiment, gives results closer to the experimental values[105], suggesting that the significance of the biphotonic model may be pronounced for $\epsilon_1 \prec\prec \epsilon_2$. In addition, calculations are also made for conditions (i)-(ii) with k_{2B}/k_{1B} changes from 0.26 to 0.50, and the results are also similar[105].

iv) <u>The Calculated Results from Model I</u>

The interpretation of the data made here is a follow-up to the above-mentioned results obtained from Model

I. Applications of a kinetic model(Model I) generate the calculated(theoretical) k_{1B} and k_{2B} values.

As seen in Table 3.2, theoretical k_{2B}(calc.) and experimental k_{2B}(expt.) values, which show greater agreement within ± 0.1 x 10^{-2} s^{-1} for each polymer matrix used, are within the experimental error of the **E** → **C** reaction[46].

Generally, the following interpretations bear relevance to the considerations discussed previously. For nonpolar media(PS and PTBS), the k_{1B}(calc.) for PTBS is 9.2 x 10^{-2} s^{-1} which is greater than the k_{1B}(calc.) for PS of 2.9x 10^{-2} s^{-1}. This may be due to the extra free volume at the dye site for PTBS than PS. Meanwhile, the rate constants(k_{1B}) in dipolar media(PNBMA and PVAC) are comparable, but slightly greater than those in nonpolar medium such as PS. The k_{1B}(calc.) for PNBMA is 4.7 x 10^{-2} s^{-1}, whereas k_{1B}(calc.) for PVAC is 4.9 x 10^{-2} s^{-1}. The main aspect of such results to focus on is the fact that, at the reaction temperature of 303 K, the T_gs of PVAC(302 K) and PNBMA(307 K) are well below the T_g of PS(373 K)[11]. Perhaps the main chain molecular motions near the T_g of the polymer facilitate the photoisomerization even though the possibility of the cooperative motions(between dye and medium) in controlling the reaction rate cannot be ignored. Interestingly, k_{1B} values for dipolar PNBMA and PVAC are slightly less than k_{1B} for nonpolar PTBS. The plausible presence of weak dipolar interactions of the molecules, between the dipolar medium and the dye(**Z** form), may stabilize

the dye and thus retard the reaction. On the whole, the k_{1B}(calc.) for the photoisomerization **Z** → **E** is greater than k_{2B}'s for **E** → **C** by a factor of 2-4 for all the matrices. The real reasons for such observations are unknown. Perhaps, during photoisomerization, the process of breaking of the π-bond(connecting between the α-C of the ethylidene and C of succinic anhydride), followed by rotation around the C-C bond and the reformation of the π-bond, is faster than the photoinduced ring-closure reaction, **E** → **C**, which involves the forming of a new σ-bond accompanied by the rearrangement of two π-bonds[46]. In addition, there may be sufficient free volume at the dye site for the photoisomerization of **Z** → **E** to take place although in the **Z** → **E** reaction the furan moiety requires extra free volume to form the **E** form. However, in the **E** → **C**, that extra free volume of the same moiety is much less[105].

As expected for the photoinduced reaction **Z** → **E**, the apparent thermal activation energies, E_a, are small, as shown in Table 3.3. E_a is a function of E_0, E_η and E_s[96,101,109]. E_0, E_η and E_s are intrinsic activation energy, activation energy due to viscosity and activation energy due to solvation respectively. Note that E_s is a measure of the degree of interactions between the medium and the solute which contribute to the change in the energy barrier[96,101].

C Photobleaching of **C** → **E** of Aberchrome 540 in Solid Polymer Matrices at Low Temperatures

Each of the first-order plots, as seen in Figures 3.22-3.49, gives two distinct lines, one after another, suggesting the plausible existence of more than one process. It is worth noting that the k_{2C} represents the apparent rate constants after approximately 2-5 minutes of the irradiation times for PS and about 1-2 minutes for PC. For the reactions which involve thinner sample mixtures(mixtures of dye and polymer in solvent for casting sample films), it takes approximately 0.25-0.6 minutes of the irradiation times for both PS and PC to reach maximum conversions, leading to the extraction of k_{2C}.

At such cryogenic temperatures, the movement of the guest(dye) molecules in a rigid polymer matrix is restricted[30]. If there is inadequate free volume at the dye sites, then the deviation from the first-order plot, which is observed in the thermal bleaching of merocyanine to spiropyran[34,36], should have been observed in the present work. It seems that the polymer matrix does not interact with the dye(**C** form) strongly. The only evidence of some weak interactions between the dye and the dipolar polymer is found[10-11]. A general trend shows that the rate constants, k_{2C}, in non-dipolar(PS) and in dipolar medium(PC), differ by a factor of 2-4. For example, at 303 K, the rate constants, k_{2C} of the dye reaction in PS is 4.2×10^{-2} s^{-1} and in

PC is 8.0 x 10^{-2} s^{-1}. Extra free volume at the dye sites created by the bulkier and less flexible unit of PC may account for such differences. This is reflected in the apparent activation energies in PS and PC. The activation energy for the dye reaction in PC(Ea=0.6 kJ mol^{-1}) is smaller than that in PS(Ea=1.5 kJ mol^{-1}).

The Arrhenius equation is usually applicable to relaxation in amorphous polymers like PS and PC, occurring at subglass transition temperatures(β and γ relaxations) and at a glass-rubber temperature(α relaxation). The α relaxation results from a large-scale conformational rearrangement of the polymer main-chain segmental backbone motion. The loss peak corresponding to α relaxation is observed at a temperature around and above T_g. On the other hand, the secondary loss regions(β and γ relaxations) result from motions within the polymer(due to side groups)[85].

In the present work, the temperature range studied is between 83-303 K, which is well below the T_gs for PS(373 K) and PC(418 K). Therefore, the molecular motions in PS and PC at such low temperatures cannot be from the main-chain. Hence the detail mechanisms for the molecular motions related to the β and γ relaxation effects in PS and PC are discussed herein.

i) <u>β and γ relaxations</u>

For photodecolouration in PS and PC, two single straight lines for the Arrhenius plots are obtained as seen in

Figures 3.50-3.51. It is more likely that below the T_g, there is a change in the polymer matrix around the subglass transition temperature. Consequently, the rate of photodecolouration of the dye is affected by the change in matrix. Such a change brings about the gradual change in the slope of the Arrhenius plot.

One of the pieces of evidence to support the above point(that the dye reaction could be occurring in two different micro-environments) may be obtained from the mechanical and dielectric relaxation of PS[110]. Three subglass transition temperatures have been identified. A β transition involves the local motion of chain segments including phenyl rings. The γ and δ transitions dominate at sub-ambient temperatures and may be caused by the phenyl ring rotation and wagging. The change in the matrix which seems to have a direct influence on the rate of photobleaching of the dye is shown in Figure 3.50.

PC is well known to show a large local relaxation process at 150-170 K called γ transition[40,111-112].

The Arrhenius plot in Figure 3.51 shows a γ transition temperature at 203 K. The results of two different systems, i.e. neutron scattering[113] and dynamic mechanical measurement[114], reveal that the molecular motion due to the γ relaxation is attributed to the relaxation of the monomer units as a whole. In addition, the intermediate β relaxation is probably due to packing defects in the glassy state[111].

The lower value of the present γ transition temperature from the usual literature value(150-170 K)[40,111-112] may be caused by the different time scale of the present measurements and/or the different in the degree of crystallinity of the PC samples. The presence of different microenvironments, which correspond to the gradual change in the slope of the Arrhenius plot shown in Figure 3.51, is obviously following the above-mentioned pattern.

ii) Problems Associated with the Solution-cast Technique

In the solution-cast technique involving the polymer thin solid film, applied to this current work, two problems are of primary concern. The first is the effect of the dye concentration on the rate constant, and the second is the inhomogeneity of the dispersed dye in a thin polymer film. To check whether the observed apparent rate constant is independent of the dye concentration, the reaction was obtained by increasing the dye concentration by a factor of 1.5 to get these sets of k_{1C} values. The second problem observed during the polymer films preparation was a slight inhomogeneity in the distribution of the dispersed dye near the edges of the quartz plates caused by the uneven intermolecular forces(near the edges) as compared to the central region of the plate. As a result, only the central region of each plate was used for the study because of the uniformly distributed dye located in the central region.

4.2 Conclusion

In the course of this investigation, several important results are presented. The kinetics of the photocolouration of the amber **E** form in various solvents and the photobleaching of the red **C** form of Aberchrome 540 in a number of polymer matrices follow a simple first-order process at the temperature range investigated. In the former case, the dye reaction in the photocolouration studies show one first-order process. Various factors affecting the rate constant have been discussed, i.e. the effects of polarity of the medium, viscosity effect of the solvent, reaction temperature, and hydrogen bonding effect. The hydrogen bonding formation is more likely to influence the rate constants of the dye reaction. In the studies of photobleaching of the red **C** form in PS and PC at low temperatures, the kinetics follow two first-order processes, one after another, suggesting the presence of two different types of dye sites in the polymer matrix. In addition, various modes of molecular motions of media(β and γ relaxations) affecting the kinetics have been discussed. Meanwhile, in a kinetic study of photoisomerization **Z** → **E**, the absorption spectra of **Z** and **E** forms are similar and cannot then be used to monitor the progress of the reaction. Only the coloured **C** form, which is generated as the final product, is used. Two theoretical kinetic models are used to simulate the experimental data using the known k_{2B} obtained

previously[46]. The first model has an advantage because it requires less assumptions for data evaluation. The second model, also known as a biphotonic model, considers the effect of competition for the photons by the reactants in the dye reaction. The biphotonic model is difficult to apply. It requires several assumptions and is only applicable at a low conversion factor. In spite of these drawbacks, the biphotonic model does show[105] the relative yields of the product, which follow the general trends of the experimental data, although the model slightly underestimates the product yields.

The unique photoinduced reactions in the present work are of special interest, since in the mostly studied thermal bleaching of the colored merocyanine to spiropyran in PMMA, nonlinearity of the first-order plot is observed along with the possible existence of several conformers of merocyanine. Various conformers of merocyanine can react simultaneously at increasing exposure times, resulting in nonlinearity in the first-order plot. However, the latter may also be caused by the matrix effect restricting the dye molecular motions in the course of photoisomerization. It is worth noting that there is no single factor involved that can rationalize the kinetic differences in the photoinduced reactions of Aberchrome 540(E form) and merocyanine. Two main considerations affecting the reaction pathways of both types of photochromic compounds should not be neglected: firstly,

coloured merocyanine is zwitterionic but the amber **E** form of Aberchrome 540 is neutral, and secondly, the size of merocyanine is somewhat larger than that of **E** form. As a consequence, merocyanine dye requires more critical free volume to undergo a photochemical reaction. Hence, matrix effect, which plays a vital role in controlling its reaction kinetics, may also be the cause for such deviation from linearity of the first-order plot.

4.3 Possible Future Developments and Suggestions for Further Work

Research aimed at a deeper understanding of the roles of the charges, the size of the photochromic probe, and their influences on the reaction chemical kinetics of a photoinduced reaction would be beneficial to the present work.

The present photocolouration study from **E** → **C** is done in non-restricted media such as various solvents with different polarity to examine their influence on photochromic behaviour. Perhaps future studies should be done to investigate the effects of polarity, viscosity, and hydrogen bonding on the rate of the dye reaction, e.g. a set of isoviscous solvents(or their mixtures) with a varying polarity should be studied independently to isolate the polarity effect from the composite effects[115]. Thus, further valuable insight on the dipolar interactions(dye and the medium) could be obtained.

It is expected that the availability of more basic information on the kinetics and the reactions of photochromic compounds should help improving the designs of e.g. a high density optical data storage, electro-optic devices, etc.

5 REFERENCES

[1] G. H. Brown(ed.), ***Photochromism***, p.6, Wiley-Interscience, New York(1971).

[2] H. Morrison and R. M. Deibel, ***Photochem. Photobiol.***, ***43***, 663(1986).

[3] H. J. C. Jacobs and E. Havinga, ***Adv. Photochem.***, ***11***, 305(1979).

[4] H.Dürr and H. Bouas-Laurent(eds), ***Photochromism, Studies in Organic Chemistry 40***, Elsevier, Amsterdam(1990).

[5] E. ter Meer, ***Justus Liebigs Ann. Chem.***, ***181***, 1(1876).

[6] W. S. Johnson and G. H. Daub, ***Org. Reactions, 6***, ch. 1(1951).

[7] C. B. McArdle(ed.), ***Applied Photochromic Polymer Systems***,pp.80-120, Blackie, Glasgow(1992).

[8] H. Stobbe, ***Justus Liebigs Ann. Chem.***, ***380***, 1(1911).

[9] H. G. Heller, P. J. Darcy, P. J. Strydom, and J. Whittal, ***J. Chem. Soc., Perkin Trans. 1***, 202(1981).

[10] M. Rappon, R. T. Syvitski, and A. Chuenarm, ***Eur. Polym. J.***, ***28***, 399(1992).

[11] M. Rappon, A. Chuenarm, A. J. Duggal, H. Gill, O. Bhaovibul, R. T. Syvitski, ***Eur. Polym. J.***, ***27***, 365(1991).

[12] Z. F. Liu, K. Hashimoto, and A. Fujishima, ***Nature***, ***347***, 658(1990).

[13] S. Tazuke, ***Jpn. J. Appl. Phys. suppl. 26-4***, ***26***,

3(1987).

[14] G. H. Dorion and A. F. Wiebe, ***Photochromism, Optical and Photographic Applications*** , Focal Press, London(1979).

[15] S. Tazuke, S. Kurihara, H. Yamaguchi, and T. Ikeda, ***J. Phys. Chem.***, ***91***, 249(1987).

[16] W. E. Moerner, ***Jpn. J. Appl. Phys. suppl. 3***, ***28***, 221(1989).

[17] Y. Yokoyama, T. Yamane, Y. Kurita, ***J. Chem. Soc., Chem. Commun.***, 1722(1991).

[18] M. Irie, O. Miyatake, and K. Uchida, ***J. Amer. Chem. Soc.***, ***114***, 8715(1992).

[19] B. Batchelor and N. Stephens, ***Proc. SPIE - Int. Soc. Opt. Eng.***, ***2055***, 310(1993).

[20] J. C. Crano, C. N. Welch, B. V. Gemert, D. Knowles, and B. Anderson, ***Spec. Publ. - R. Soc. Chem.***(Photochemistry and Polymeric Systems), ***125***, 179(1993).

[21] M. Uchida and M. Irie, ***Chem. Lett.***, ***12***, 2159(1991).

[22] S. Tamura, N. Asai, and J. Seto, ***Bull. Chem. Soc. Jpn.***, ***62***, 358(1989).

[23] Y. Yokoyama, H. Hayata, H. Ito, and Y. Kurita, ***Bull. Chem. Soc. Jpn.***, ***63***, 1607(1990).

[24] M. Usui, T. Nishiwaki, K. Anda, and M. Hida, ***Chem. Lett.***, 1561(1984).

[25] Y. Nakayama, K. Hayashi, and M. Irie, ***Bull. Chem.***

Soc. Jpn., ***64***, 789(1991).

[26] Y. Hirshberg, ***J. Amer. Chem. Soc.***, ***78***, 2304(1956).

[27] H. G. Heller, ***IEE Proc.***, ***130***, pt. I, 209(1983).

[28] G. J. Ashwell(ed.), ***Molecular Electronics***, Research Studies Press, Taunton(1991).

[29] D. A. Parthenopoulos and P. M. Rentzepis, ***Science***, ***245***, 843(1989).

[30] R. J. H. Clark and R. E. Hester(eds), ***Spectroscopy of New Materials***, pp.61-85, John Wiley, New York(1993).

[31] P. Bamfield(ed.), ***Fine Chemicals for the Electronics Industry***, pp.120-135, The Royal Society of Chemistry, Burlington House, London(1986).

[32] B. Batchelor and N. Stephens, ***Proc. SPIE - Int. Soc. Opt. Eng.***, ***2055***, 310(1993).

[33] V. Krongauz, ***Mol. Cryst. Liq. Cryst.***, ***246***, 339(1994).

[34] Z.G. Gardlund, ***J. Polym. Sci.; Polym. Lett.***, ***6***, 57(1968).

[35] M. Kryszewski, D. Lapienis, and B. Nadolski, ***J. Polym. Sci.; Polym. Chem. Edn.***, ***11***, 2423(1973).

[36] M. Kryszewski, B. Nadolski, A. M. North, and R. A. Pethrick, ***J. Chem. Soc.; Faraday Trans. II***, ***76***, 351(1980).

[37] G. Smets, J. Theon, and A. Aerts, ***J. Polym. Sci.; Polym. Symp.***, ***51***, 119(1975).

[38] J. Verborgt and G. Smets, ***J. Polym. Sci.; Polym. Chem. Edn.***, ***12***, 2511(1974).

[39] K. Horie, K. Hirao, N. Kenmochi, and I. Mita, ***Makromolek. Chem.; Rapid Commun.***, ***9***, 267(1988).

[40] K. Horie, M. Tsukamoto, and I. Mita, ***Eur. Polym. J.***, ***21***, 805(1985).

[41] N. G. Lawrie and A. M. North, ***Eur. Polym. J.***, ***9***, 345(1973).

[42] T. Seki and K. Ichimura, ***Macromolecules***, ***23***, 31(1990).

[43] P. Uznański, A. Wojda, and M. Kryszewski, ***Eur. Polym. J.***, ***26***, 141(1990).

[44] W. J. Priest and M. M. Sifain, ***J. Polym. Sci.***, Part A-1, ***9***, 3161(1971).

[45] T. Tsutsui, A. Hatakeyama, and S. Saito, ***Chem. Phys. Lett.***, ***132***, 563(1986).

[46] M. Rappon and K. M. Ghazalli, ***Eur. Polym. J.***, ***31***, 233(1995).

[47] G. Smets, ***Adv. Polym. Sci.***, ***50***, 17(1983).

[48] K. Horie and I. Mita, ***Adv. Polym. Sci.***, ***88***, 77(1989).

[49] J. L. R. Williams and R. C. Daly, ***Prog Polym. Sci.***, ***5***, 61(1977).

[50] W. C. Yu, C. S. P. Sung, and R. E. Robertson, ***Macromolecules***, ***21***, 355(1988).

[51] T. Naito, K. Horie, and I. Mita, ***Eur. Polym. J.***, ***26***,

1295(1990).

[52] T. Naito, K. Horie, and I.Mita, ***Macromolecules***, ***24***, 2907(1991).

[53] J. G. Victor and J. M. Torkelson, ***Macromolecules***, ***20***, 2241(1987).

[54] J. Liu, Q. Deng, and Y. C. Jean, ***Macromolecules***, ***26***, 7149(1993).

[55] H. H. Song and R. J. Roe, ***Macromolecules***, ***20***, 2723(1987).

[56] S. Nojima, R. J. Roe, D. Rigby, and C. C. Han, ***Macromolecules***, ***23***, 4305(1990).

[57] G. G. Cameron, I. S. Miles, and A. Bullock, ***Br. Polym. J.***, ***19***, 129(1987).

[58] D. W. McCall, ***Acc. Chem. Res.***, ***4***, 223(1971).

[59] J. Naciri and R. G. Weiss, ***Macromolecules***, ***22***, 3928(1989).

[60] Y. Ishida, ***J. Polym. Sci.***, Pt A-2, ***7***, 1835(1969).

[61] M. H. Cohen and D. Turnbull, ***J. Chem. Phys.***, ***31***, 1164(1959).

[62] D. Turnbull and M. H. Cohen, ***J. Chem. Phys.***, ***34***, 120(1961).

[63] G. S. Crest, M. H. Cohen, ***Adv. Chem. Phys.***, ***48***, 455(1981).

[64] R. Simha and T. Somcynsky, ***Macromolecules***, ***2***, 342(1969).

[65] T. Somcynsky and R. Simha, ***J. Appl. Phys.***, ***42***,

4545(1971).

[66] S. Misra and W. L. Mattice, ***Macromolecules, 26,*** 7274(1993).

[67] C. Lenoble and R. S. Becker, ***J. Phys. Chem., 90,*** 62(1986).

[68] Y. Kalisky and D. J. Williams, ***Macromolecules, 17,*** 292(1984).

[69] Y. Kalisky, T. E. Oriowski and D. J. Williams, ***J. Phys. Chem., 87,*** 5333(1983).

[70] J. Malkin, A. S. Dvornikov, and P. M. Rentzepis, ***Proc. SPIE - Int. Soc. Opt. Eng., 1853,*** 163(1993).

[71] E. V. Bystritskaya, T. S. Karpovich, and O. N. Karpukhin, ***Dokl. Phys. Chem., 228,*** 632(1976).

[72] R. Richert and H. Bässler, ***Chem. Phys. Lett., 116,*** 302(1985).

[73] R. Richert, ***Chem. Phys. Lett., 118,*** 534(1985).

[74] K. Hirao, K. Horie, and I. Mita, ***Polym. Prep. Jpn., 34,*** 1573(1985).

[75] C. S. P. Sung, I. R. Gould, and N. J. Turro, ***Macromolecules, 17,*** 1447(1984).

[76] M. Miura, T. Hayashi, F. Akutsa, and K. Nagakubo, ***Polymer, 19,*** 348(1978).

[77] C. S. Paik and H. Morawetz, ***Macromolecules, 5,*** 171(1972).

[78] V. Deblauwe and G. Smets, ***Makromol. Chem., 189,***

2503(1988).

[79] T. Tsuruta, M. Doyama, and M. Seno(eds), ***New Functionality Materials, Volume C: Synthetic Process and Control of Functionality Materials***, p. 357, Elsevier, Amsterdam(1993).

[80] Y. Yoshioka, T. Tanaka, M. Sawada, and M. Irie, ***Chem. Lett.***, 19(1989).

[81] H. G. Heller and M. Szewczyk, ***J. Chem. Soc., Perkin Trans. 1***, 1487(1974).

[82] C. Lenoble and R. S. Becker, ***J. Phys. Chem., 90***, 2651(1986).

[83] L. Yu, Y. Ming, and M. Fan, ***Res. Chem. Intermed., 19***, 829(1993).

[84] Z. Yoshida and T. Kitao(eds), ***Chemistry of Functional Dyes***, Mita, Tokyo(1989).

[85] N. G. McCrum, B. E. Read, and G. Williams, ***Anelastic and Dielectric Effects in Polymeric Solids***, Wiley, London(1967).

[86] C. Reichardt, ***Solvents and Solvent Effects in Organic Chemistry***, 2nd ed., VCH, Weinheim(1988).

[87] E. L. McCaffery, ***Laboratory Preparation for Macromolecular Chemistry***, pp.149-153, McGraw-Hill, New York(1970).

[88] J. Brandrup and E. H. Immergut, ***Polymer Handbook***, 3rd Edn., John Wiley, New York(1989).

[89] H. G. Heller and J. R. Langan, ***J. Chem. Soc., Perkin***

Trans. 2, 341(1981).

[90] M. Rappon, ***Eur. Polym. J.***, ***22***, 319(1986).

[91] M. Rappon(formerly Rujimethabhas) and N. A. Weir, ***Eur. Polym. J.***, ***19***, 779(1983).

[92] M. Rappon and N. A. Weir, ***Eur. Polym. J.***, ***18***, 813(1982).

[93] M. N. Jirmanus, ***Introduction to Laboratory Cryogenics***, Janis Research Co., Wilmington, Massachusetts(1990).

[94] I. Mita, K. Horie, and K. Hirao, ***Macromolecules***, ***22***, 558(1989).

[95] I. Mita, T. Naito, and K. Horie, ***J. Photopolym. Sci. Technol.***, ***1***, 303(1988).

[96] M. Rappon, R. T. Syvitski, and K. M. Ghazalli, ***J. Mol. Liq.***, ***62***, 159(1994).

[97] C. D. Eisenbach, ***Ber. Buns. Phys. Chem.***, ***84***, 680(1980).

[98] N. S. Park and D. H. Waldeck, ***J. Phys. Chem.***, ***94***, 662(1992).

[99] G. van der Zwan and J. T. Hynes, ***Chem. Phys.***, ***90***, 21(1984).

[100] J. Hicks, M. Vandersall, Z. Babarogic, and K. B. Eisenthal, ***Chem. Phys. Lett.***, ***116***, 18(1985).

[101] J. M. Hicks, M. T. Vandersall, E. V. Sitzmann, and K. B. Eisenthal, ***Chem. Phys. Lett.***, ***135***, 413(1987).

[102] W. Klemperer, ***Science***, ***257***, 887(1992).

[103] P. Nicolet, C. Laurence, and M. Lucon, ***J. Chem. Soc., Perkin Trans. 2***, 483(1987).

[104] L. J. Bellamy, ***The Infrared Spectra of Complex Molecules***, vol. 2, 2nd Edn., Chapman and Hall, London(1980).

[105] M. Rappon and K. M. Ghazalli, ***Eur. Polym. J.*** (In press).

[106] L. Z. Vinogradov, A. A. Krasheninnikov, and A. B. Shablia, ***Z. Prikl. Spektros., 50***, 50(1989).

[107] G. Bergamsco, P. Calvelli, and R. Polloni, ***Opt. Quant. Electro., 25***, 859(1993).

[108] D. L. Andrews, D. P. Craig, and T. Thirunamachandran, ***Int. Rev. Phys. Chem., 8***, 339(1989).

[109] D. H. Waldeck, ***J. Mol. Liq., 57***, 127(1993).

[110] P. Hedvig, ***Dielectric Spectroscopy of Polymers***, pp. 113-119, Wiley & Sons, New York(1977).

[111] A. F. Yee and S. A. Smith, ***Macromolecules, 14***, 54(1981).

[112] M. Kochi, T. Sasaki, and H. Kambe, ***Polym. J., 10***, 169(1978).

[113] G. Floudas, J. S. Higgins, G. Meier, F. Kremer, and E. W. Fischer, ***Macromolecules, 26***, 1676(1993).

[114] J. Y. Jho and A. F. Yee, ***Macromolecules, 24***, 1905(1991).

[115] M. Rappon and R. T. Syvitski, ***J. Photochem. and***

Photobiol. A(Accepted for publication, 1995).

6 APPENDICES

APPENDIX A GLOSSARY OF SYMBOLS

SYMBOL	DEFINITON WITH UNIT	EXPERIMENTAL SECTION
A	Arrhenius preexponential factor	3(ii)
c	Concentration of absorbing molecules, $molL^{-1}$	3(iii)
E_a	Activation energy, $kJ\ mol^{-1}$	3(ii)
I	Intensity of transmitted light, $photon.s^{-1}$	3(iii)
I_o	Intensity of incident light, $photon.s^{-1}$	3(iii)
k	Reaction rate constant, s^{-1}	General
ℓ	Absorbing pathlength, cm	3(iii)

SYMBOL	DEFINITON WITH UNIT	EXPERIMENTAL SECTION
M	Molecular weight	2.1(B)
N	Avogadro's number, 6.023×10^{23} mol^{-1}	3(iii)
R	Molar gas constant, 8.314 $JK^{-1}mol^{-1}$	3(ii)
T_g	Glass-transition temperature, K	General
ϵ	Molar absorption coefficient, $dm^3mol^{-1}cm^{-1}$	3(iii)
Φ	Quantum yield	General
λ	Wavelength of light, nm	General

APPENDIX B STRUCTURES OF SOME COMMON POLYMERS USED IN THIS WORK

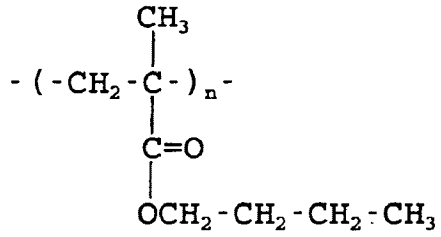

poly(n-butyl methacrylate)(PNBMA)

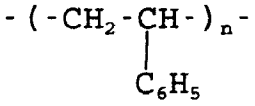

poly(styrene)(PS)

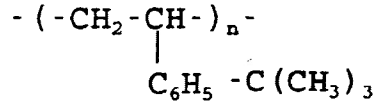

poly(p-tert-butyl styrene)(PTBS)

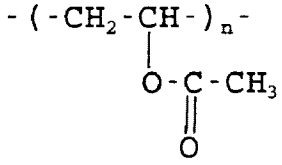

poly(vinyl acetate)(PVAc)

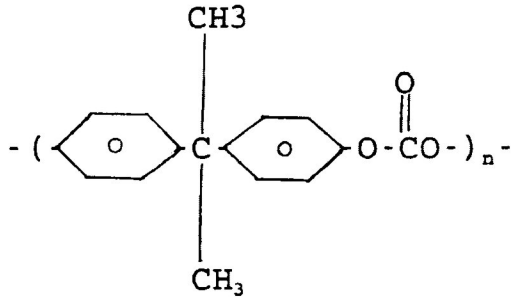

poly(carbonate bisphenol A)(PC)

APPENDIX C THEORETICAL FORMULATION FOR BIPHOTONIC MODEL: MODEL II

For **Z → E → C** reaction,

$$\frac{dE}{dt}=k_{1B}I_1Z-k_{2B}I_2E---(C1),\ where$$

I_1 and I_2 are the intensities of the first and second photons respectively. Note that Z + E + C = Z_0; thus at any given time, t,

$$Z=Z_0-E-C.$$

Substitution of the above expression for (C1) results in

$$\frac{dE}{dt}=k_{1B}I_1[Z_0-E-C]-k_{2B}I_2E---(C2).$$

At a photostationary state, dE/dt=0. Hence, the solution for E gives

$$E=\frac{k_{1B}I_1Z_0-k_{1B}I_1C}{k_{1B}I_1+k_{2B}I_2}---(C3).$$

For expression (C3), it may be assumed that, for small value C which is valid at the beginning of the reaction, C ≈0. Then equation (C3) is simplified to

$$E=\frac{k_{1B}I_1Z_0}{k_{1B}I_1+k_{2B}I_2}---(C4).$$

C may be expressed as

$$C=k_{2B}\int_0^t I_2 E dt,$$

with the insertion of E from equation (C4), to become

$$C=k_{2B}\int_0^t I_2\left[\frac{k_{1B}I_1Z_0}{k_{1B}I_1+k_{2B}I_2}\right]dt,$$

which on rearrangement gives

$$\frac{C}{Z_0}=k_{2B}\int_0^t\left[\frac{I_1I_2}{I_1+\left(\frac{k_{2B}}{k_{1B}}\right)I_2}\right]dt---(C5).$$

It is worth mentioning that $I_1, I_2=f(\lambda, t)$. There is no analytic solution for equation (C5) because of the unknown intensities of I_1 and I_2(originating from the same incident intensity, I_0, changing with the simultaneous changes in wavelength of light, λ, and time, t). The exact analytic solution cannot be found. As a result, the following simplifying assumptions are

required:

a) I_1 and I_2 are independent of λ;

b) the individual intensity of I_1 and I_2 is proportional to the intensity of light absorbed[I_{abs}] by Z and E respectively. Presumably, the proportionality constant is K, thus expressions for I_1 and I_2 are described as $I_1=KI_{abs,Z}$, and $I_2=KI_{abs,E}$, where I at ℓ equals to $I_0e^{-2.303\epsilon\ell[X]}$. ϵ is the molar absorptivity, ℓ is the pathlength, and [X] is the concentration of the chemical X.

Now,

$$I_1=K(1-e^{-2.303\epsilon_1 lZ})\,I_0,$$

and

$$I_2=K(1-e^{-2.303\epsilon_2 lE})\,I_0.$$

When $2.303\epsilon_1\ell Z<1$ and $2.303\epsilon_2\ell E<1$, then the exponential terms may be expanded and equation (C5) becomes

$$\frac{C}{Z_0}=k_{2B}\int_0^t\left[\frac{(2.303\epsilon_1 lZI_0K)\,(2.303\epsilon_2 lEI_0K)}{(2.303\epsilon_1 lZI_0K)+\left(\frac{k_{2B}}{k_{1B}}\right)(2.303\epsilon_2 lEI_0K)}\right]dt$$

$$=2.303k_{2B}I_0lK\int_0^t [\frac{(\epsilon_1 Z)\ (\epsilon_2 E)}{\epsilon_1 Z + (\frac{k_{2B}}{k_{1B}})\epsilon_2 E}]\, dt.$$

This derivation is further simplified by assuming, at the photostationary state that E is constant with respect to time and Z changes very little during that time, giving rise to

$$\frac{C}{Z_0} = 2.303k_{2B}I_0lK[\frac{(\epsilon_1 Z)\ (\epsilon_2 E)}{\epsilon_1 Z + (\frac{k_{2B}}{k_{1B}})\epsilon_2 E}]\int_0^t dt$$

or

$$\frac{C}{Z_0} = 2.303k_{2B}Z_0I_0lK[\frac{(\epsilon_1 Z)\ (\epsilon_2 E)}{\epsilon_1 Z + (\frac{k_{2B}}{k_{1B}})\epsilon_2 E}]\, t \text{---} (C6),$$

where C/Z_0 defines the ratio of the concentration of C formed relative to the total initial concentration of Z. For a given experiment, the known constant values are from the parameters of Z_0, I_0 and ℓ, and k_{2B}(from previous **E** → **C** work[46]). Only k_{1B}

and time,t, vary. To examine the effect of change in k_{1B} on the yield, the term in the closed brackets x t(equation (C6)) is computed and is normalized against the largest value to obtain the calculated normalized ratio,C/Z_0 seen earlier.

APPENDIX D COMPUTER PROGRAMS FOR SELECTED EXPERIMENTS

This APL*PLUS system software generated program ABR, which was used to calculate the value of R(absorbance ratio, A_t/A_∞) experimentally.

```
     ▽ABR[□] ▽
[0]  ABR;N;T;A;I;R
[1]  'ENTER NAME OF POLYMER AND TEMP, N'
[2]  N ← □
[3]  'AT THE TEMPERATURE, T'
[4]  T ← □
[5]  'ENTER ABSORBANCE IN ORDER OF INCREASING TIME, A'
[6]  A ← □
[7]  'ENTER ABSORBANCE AT TIME INFINITY, I'
[8]  I ← □
[9]  R ← A ÷ I
[10] 1 □POKE 116
[11] 'HERE ARE THE RESULTS OF, N'
[12] ' '
[13] N
[14] 'AT TEMP, T'
[15] ' '
[16] T
[17] 'WITH RATIOS, R'
[18] ' '
[19] R
[20] 'FOR A'
[21] ' '
[22] A
[23] 'FOR I'
[24] ' '
[25] I
[26] 0 □POKE 116
```

This APL program known as PHOTO2 was used to collect the chemical data for the normalized ratio C/Z_0.

```
▼PHOTO2[□]▼
[0]PHOTO2
[1]B ← ⍳25
[2]A ← 100-B
[3]'PUT IN VALUE OF E1'
[4]E1 ← □
[5]'PUT IN VAL OF E2'
[6]E2 ← □
[7]'PUT IN VAL. OF RATIO K2B/K1B ← L'
[8]L ← □
[9]F ← AxE1
[10]G ← BxE2
[11]H ← LxG
[12]R ←(FxG)÷(F+H)
[13]P ← R ÷ ⌈/R
[14]'HERE ARE THE VALUES OF R'
[15]R
[16]' '
[17]'HERE ARE THE NORMALIZED R IE P'
[18]P
[19]' '
[20]O □POKE 116
```

This c-programming language, KINFIT, was set up to calculate the value of the absorbance ratio, A_t/A_∞ to provide the best fit to the experimental data.(Note: k_1 and k_2 used in this program KINFIT are referred to k_{1B} and K_{2B} in the text).

```
#include <stdio.h>
#include <math.h>

main()
{ int i,j, n_pointi, jmax;
f l o a t    t [ 8 0 ] ,    t m i n ,    t m a x ,
t_inc,A1,A2,R[80],k1[50],k2[50],arg1,arg2,c;
char name[40],kfile[50], outfile[50];
FILE *inp, *outp;

printf ("What are tmin, tmax, t_inc ? \n");
scanf("%f %f %f", &tmin, &tmax, &t_inc);
  printf("tmin=%f tmax=%f t_inc=%f\n ",tmin,tmax, t_inc);
printf("Name of reaction: \n");
scanf ("%s", name);

printf("Name of data file :\n");
scanf("%s", kfile);

printf("Name of output file: \n");
scanf("%s", outfile);

inp = fopen (kfile, "r");
j=0;
 while ((fscanf(inp,"%f %f", &k1[j], &k2[j])) !=EOF)
j++;

jmax = j-1;
/* it is important to have this j-1, if not it reads wrong
last value*/

fclose(inp);
outp = fopen(outfile, "w");
fprintf(outp, "Results of t & R of %s\n", name);
t[0] = tmin;
n_pointi = (tmax-tmin)/t_inc;

for (j=0; j<= jmax; j++)
{
c = 1/(k2[j] -k1[j]);
fprintf(outp, "\nk1 =%.3f\t k2 = %.3f\t c =%f\n",
```

```
k1[j],k2[j],c);
fprintf(outp, "t\t R\n");

for(i = 0; i<= n_pointi; i++)
{
arg1 = -k1[j]*t[i];
arg2 = -k2[j]*t[i];

A1 = k2[j]* (1- exp(arg1));
A2 = k1[j]* (1- exp(arg2));
/*A1 = k2[j]*(1- arg1);*/
/*A2 = k1[j]*(1 - arg2);*/

R[i] = c*(A1 - A2);

fprintf (outp, "%f\t %f\n ",t[i], R[i]);

t[i+1] = t[i] + t_inc;
  }
}
fclose(outp);
}
```

This APL program, REG was used to calculate the linear regression for all the plots used in this work.

```
▼REG[□]▼
[0]REG;A;B;S;I;N;P;Q1;R;D;A1;T;C;U;V;X2;Y2;W;V1;U1
[1]'ENTER THE SAMPLE NAME W'
[2]W ← □
[3]A REGRESSION Y=(S+-A)X + (I+-B)
[4]'ENTER THE VALUES OF X'
[5]X ← □
[6]'ENTER THE VALUES OF Y'
[7]Y ← □
[8]→(((⍴X)-(⍴Y))=0)/10
[9]'VECTORS OF EQUAL LENGTH REQUIRED',→ 6
[10]N ← ⍴X
[11]P ← +/XxY
[12]Q1 ← +/X
[13]Q2 ← +/Y
[14]R ← +/X*2
[15]S ← ((NxP)- Q1xQ2)÷(NxR)-Q1*2
[16]I ← ((Q2xR)-Q1xP)÷(NxR)-Q1*2
[17]D ← (SxX)+ I-Y
[18]A1 ← (+/D*2)÷(N-2)
[19]T ← (NxR)-(Q1*2)
[20]A ← ((A1÷T)xN)*0.5
[21]B ← ((A1÷T)xR)*0.5
[22]U ← Q1÷⍴X
[23]V ← Q2÷⍴Y
[24]X2 ← X-U
[25]Y2 ← Y-V
[26]C ← (+/X2xY2)÷((+/X2*2)x(+/Y2*2))*0.5
[27]1 □POKE 116
[28]'ANALYSIS RESULTS FOR'
[29]' '
[30]W
[31]'FOR X'
[32]' '
[33]X
[34]' '
[35]'AND Y'
[36]' '
[37]Y
[38]' '
[39]'THE SLOPE AND ERROR ARE              ',⍕S,A
[40]'THE Y-INTERCEPT AND ERROR ARE        ',⍕I,B
[41]'CORRELATION COEFFICIENT IS           ',⍕C
[42]'MEANS ARE     FOR X AND Y            ',⍕U,V
[43]0 □POKE 116
```

APPENDIX E SOURCES OF RESEARCH EQUIPMENT

ITEM	SOURCE
Cryogenic equipment	Janis Research Co., Inc., Wilmington, Massachusetts
Fibre optic bundle	Oriel Corporation, Stratford, Connecticut
Lock-in amplifier Model SR510	Stanford Research Systems, Inc., USA
Power\Energy meter Model 1825-C	Newport Corporation, Irvine, California
Spectrophotometer λ 11	Perkin-Elmer, Ueberlingen, Germany
Spectrophotometer 2000	Bausch & Lomb
Thermocouple thermometer - type K	Omega Engineering, Inc., Stamford, Connecticut
Thermostat - type 116B	The Superior Electric Co., Bristol, Connecticut
Tuned amplifier and null detector Type 1232-A	General Radio Co., Concord, Massachusetts

ITEM	SOURCE
Tungsten lamp	General Electric, Toronto, Ontario
U.V. lamp(Black Ray) B-100A	Ultraviolet Products, Inc., San Gabriel, California
Monochromator - SP 800A(no 45668)	UNICAM Instruments Ltd., England
Vacuum pump Model 25	Precision Scientific Co., Chicago

APPENDIX F SOURCE OF CHEMICALS

NAME	ALTERNATE NAME	SUPPLIER
Aberchrome 540 Z form	[(Z)-α-(2,5-dimethyl-3-furylethylidene) (isopropylidene) succinic anhydride]	Aberchromics Ltd, Cardiff, Wales
E form	[(E)-α-(2,5-dimethyl-3-furylethylidene) (isopropylidene) succinic anhyride]	-Same as above-
C form	[7,7a-dihydro-2,4,7,7,7a-pentamethylbenzo[b] furan-5,6-dicarboxylic anhydride]	-Same as above-
Acetonitrile(ACS Spectro Grade)	Methyl cyanide	Caledon Laboratories Ltd., Georgetown, Ontario
Chloroform(ACS Spectro Grade)	Trichloromethane	-Same as above-
Cyclohexane(ACS Spectro Grade)	Hexamethylene	-Same as above-
Cyclohexanol (Spectrophotometric Grade)	Hexahydrophenol	Aldrich Chemical Co., Milwaukee, Wisconsin
Ethanol(Absolute)	Ethyl alcohol	Consolidated Alcohols Ltd., Toronto, Ontario
Ethyl acetate (Spectroquality)	Acetic ester	Matheson Coleman & Bell, Norwood, Ohio
Heptane (Spectrophotometric Grade)	Dipropylmethane	Aldrich Chemical Co., Milwaukee, Wisconsin

APPENDIX F continued

NAME	ALTERNATE NAME	SUPPLIER
Methanol (Spectrophotometric Grade)	Methyl alcohol	-Same as above-
Methylene chloride (ACS Grade)	Dichloromethane	BDH, Toronto, Ontario
t-Pentanol (Spectrophotometric Grade)	t-Amyl alcohol	Aldrich Chemical Co., Milwaukee, Wisconsin
Poly(carbonate bisphenol A)	Poly(oxycarbonyloxy -1,4-phenylene isopropylidene-1,4-phenylene)	Polysciences, Inc., Warrington, Pennsylvania
Poly(n-butyl methacrylate)	Poly[1-(butoxycarbonyl)-1-methylethylene]	-Same as above-
Poly(p-t-butyl styrene)	Poly(4-tert-butyl-1-phenylethylene)	-Same as above-
Poly(styrene)	Poly(1-phenylethylene)	-Same as above-
Poly(vinyl acetate)	Poly(1-acetoxyethylene)	-Same as above-
Toluene (Spectrophotometric Grade)	Methylbenzene	Aldrich Chemical Co., Milwaukee, Wisconsin

7 PUBLICATIONS

Two papers have been published from the work related to this thesis, and one paper is in press.

Published papers:

1. M. Rappon, R. T. Syvitski, and K. M. Ghazalli. Molecular Association of Pentanols in n-Heptane IV: A Photochromic Reaction Probe, ***J. Mol. Liq.***, ***62***, 159(1994).
2. M. Rappon, and K. M. Ghazalli. Photo-Induced Reaction of Dye in Polymer Media - III. Kinetics of Photocolouration of Aberchrome 540 in Polymer Matrices, ***Eur. Polym. J.***, ***31***, 233(1995).
3. M. Rappon and K. M. Ghazalli. Photo-Induced Reaction of Dye in Polymer Media - IV. Kinetics of Photoisomerization Z → E of Aberchrome 540 in Polymer Matrices, ***Eur. Polym. J.***(in press).